On the origin of the relative stability of Zn^{II}NTA and Zn^{II}NTPA metal complexes. An insight from the IQA, IQF and π-FARMS methods.

*Paidamwoyo Mangondo and Ignacy Cukrowski**

Department of Chemistry, Faculty of Natural and Agricultural Sciences, University of Pretoria, Lynnwood Road, Hatfield, Pretoria 0002, South Africa

*Corresponding author:

E-mail: ignacy.cukrowski@up.ac.za
Landline: +27 12 420 3988
Fax: +27 12 420 4687

Abstract

Relative stability of Zn^{II} complexes with nitrilotriacetic acid (ZnNTA) and nitrilotri-3-propionic acid (ZnNTPA) was investigated. Classical analysis of individual interactions using local indices failed to explain the preferential formation of ZnNTA. This work shows that the preferential formation of ZnNTA is not due to the size of coordination 5-membered rings or the absence of the steric CH--HC contacts, as commonly considered. By combining Interacting Quantum Atoms/Fragments, IQA/IQF-defined properties implemented in the π-FARMS (Preorganized-interacting Fragment Attributed Relative Molecular Stability) method, (i) several measures of Zn^{II} 'affinity' to NTPA were shown to be consistently greater than to NTA and (ii) larger stability of ZnNTA was attributed to coordinated water molecules. Being smaller, NTA occupies less space around the metal centre. This results in less destabilised $Zn–OH_2$ coordination bonds and preorganization energy of H_2O fragments being smaller in ZnNTA. Only by summing preorganization energies (of ligand and water fragments) and binding energy between fragments (using π-FARMS method) we recovered the experimental trend. Importantly, the fundamental origin of all major energy components controlling relative stability of metal complexes was pin-pointed using the π-FARMS method.

Keywords: π-FARMS method, IQA and IQF methods, relative stability of metal complexes, preorganization and binding energies; computational chemistry.

1. Introduction

Molecular stability is both an essential and puzzling chemical phenomenon; essential because it is the central focus of most, if not all, chemistry and it is puzzling because there are numerous and often contradictory accounts explaining molecular stability. With the development and progression of computational techniques, there has been significant improvement in the measurement of molecular stability, quite often using thermodynamic constants such as the enthalpy of formation, formation (stability) constants and protonation constants. There is one important caveat associated with this information: whilst one identifies trends and patterns in the molecular stability, this cannot provide the fundamental understanding of why one molecular system is more stable than the other. The direct implication is that it is difficult to understand the phenomenon.

This does not imply that there have been no attempts at explaining these experimental trends. In fact, there have been numerous attempts that have gradually grown into two general approaches. The first approach interprets molecular stability by understanding the properties in the final structure of a molecule, primarily focusing on individual interactions (or properties). Considering trends in complex stability,[1] they have primarily been accounted for by: (i) lone-pair repulsion between electron rich donor-atoms, such as oxygen and nitrogen, (ii) steric repulsion in crowded molecular environments, (iii) coordination bond strength, (iv) the size of the central metal cation, and (v) inductive effects to a lesser degree.[2–6] The second approach attempts to understand the relative stability of molecular systems by analysing the energetic changes as the molecular system changes from one form to another.[7-10] This has been done in a variety of methods, including reaction mechanisms and energy decomposition schemes. Decomposition schemes involve breaking the molecule into either real or artificial fragments. The value of these schemes lies in the ability to recover experimental trends as determined by thermodynamic constants. Additionally, the energetic effect of the structural changes that occur when a molecule goes from the lowest to a higher energy form can be measured. While decomposition techniques are meaningful and successfully recover the experimental trends of relative stability (especially when used together), they aggregate effects into global changes; hence, they lack the resolution at atomic, interatomic and interfragment levels which are necessary to find the origin of the global phenomena observed.

Ni^{II}, Zn^{II} and Be^{II} complexes of nitrilotriacetic acid (NTA) and nitrilotri-3-propionic acid (NTPA) were the subjects of prior computational investigations.[11-14] Generally, it was concluded that the most likely cause of relative stability is due to the energetic penalty incurred

during the preorganization of the metal-ligand systems. Additionally, it was shown that analysing individual interactions (such as coordination bonds) regardless of the technique (structural, topological) could not fully explain the experimental trend. Moreover, using the Electronic Transition State with the Natural Orbital for Chemical Valence (ETS-NOCV)[7-9] scheme, it was determined that for the $[Zn^{II}NTA(H_2O)_2]^-$ and $[Zn^{II}NTPA(H_2O)_2]^-$ complexes (for simplicity, they will be represented as ZnNTA and ZnNTPA, respectively) (i) the distortion or preparation energy (energy required to preorganize the hydrated Zn^{II} fragments and the ligand fragments) was strongly destabilizing and in favour of ZnNTA, (ii) the interaction energy (the energy released when the two preorganized fragments bond to form the complex) is strongly stabilizing and in favour of ZnNTPA, and (iii) the combination of the distortion and the interaction energies was firmly in favour of ZnNTA, reaffirming that the differences in formation constants is largely due to the greater strain not only in the ligand but also in the hydrated Zn^{II} fragment of ZnNTPA.

A new methodology, the Interacting Quantum Fragments (IQF)[15]-rooted Preorganized-interacting Fragments Attributed Relative Molecular Stability protocol, or π-FARMS,[14] successfully explained the preferential formation of $[Be^{II}NTPA]^-$ relative to $[Be^{II}NTA]^-$ (they will be shown as BeNTPA and BeNTA, respectively, for simplicity) in accord with known experimental formation constants, $\log K_1$ = 9.23 for BeNTPA and $\log K_1$ = 6.84 for BeNTA.[16] By applying Interacting Quantum Atoms (IQA)[17-20]/IQF[15] concepts on the molecular fragments obtained by decomposing the overall complex formation process into two simplified processes (i.e., preorganization and binding), the methodology (i) recovered the experimental trend and (ii) identified repulsive interactions in the coordination sphere as the origin and main source of strain incurred during preorganization of the ligands. Furthermore, despite the coordination bonds being stronger in BeNTA, the overall binding was in favour of BeNTPA. It revealed that the origin of favourable binding to NTPA is linked with greater repulsion between Be^{II} metal centre and the carbon-backbone of NTA.

The focus of this work is on the Zn^{II} complexes of NTA and NTPA, where ZnNTA is preferentially formed with a difference in the $\log K_1$ values of about 5.15. For the purpose of this study, we expanded the π-FARMS methodology reported by us recently[14] to explore, on the fundamental level, the origin of the factors influencing relative stability of the two complexes. Results obtained are compared with those obtained for the Be^{II} complexes of NTA and NTPA as well as Zn^{II} complexes with these ligand studied previously[13] using QTAIM and ETS-NOCV.

2. Computational Details

The lowest energy conformers (LECs) of the ligands[14] (NTA and NTPA) and Zn^{II} complexes (ZnNTA and ZnNTPA)[13] were used for this study and, when applicable, they were re-optimized at the MP2(FC) levels of theory using the Gaussian 09 revision D.[21] Furthermore, to have the structural benefit of the MP2-structures but to minimize the computational expense when computing IQA, single point calculations (SPCs) were carried out on the MP2-optimized structures at the PBE1PBE, B3LYP and X3LYP levels of theory.

To compute the preorganization and binding energies for each complex, SPCs were performed at all levels of theory on the pre-organized, as found in the complexes, ligands, $\mathcal{L}_p$, and metal-containing fragment, $\{[Zn(H_2O)_2]^{2+}\}_p = (\mathcal{M}_w)_p$. As an example, molecular fragments obtained from two/four partitioning schemes are shown in Figure 1a/1b for ZnNTA. To obtain the free metal-containing fragment, $\{[Zn(H_2O)_2]^{2+}\}_f = (\mathcal{M}_w)_f$, the fully hydrated zinc complex, $[Zn(H_2O)_6]^{2+}$, was optimized in solvent at the MP2 level of theory. Different diaqua fragments $(\mathcal{M}_w)_f$ were generated and SPCs were performed. The lowest energy fragment was selected for computation of the preorganization energy of the metal-containing fragment.

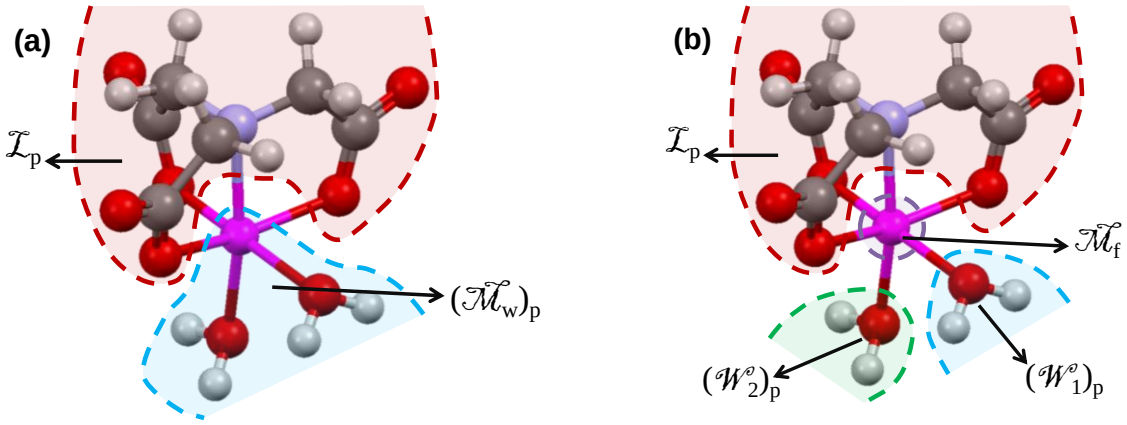

Figure 1. The fragments selected for the computation of the binding energy of metal complexes (a) a 2-component partitioning and (b) a 4-component partitioning.

Importantly, we found that the preorganization energies of the highest and lowest energy $(\mathcal{M}_w)_f$ fragments were found to be identical to the first decimal place in kcal mol^{-1}. Alternatively, when 4-component partitioning was used, Figure 1b, the binding energy was determined as the energy released when the ligand $\mathcal{L}_p$, metal centre, $\mathcal{M}_f$, and two water molecules, equatorial $(\mathcal{W}^e_1)_p$ and axial $(\mathcal{W}^e_2)_p$, form the complex. In this instance, SPCs were also required of the pre-organized water molecules and the free Zn^{2+} ion.

To assure comparability, the computational details employed here were the same as used previously in the study of Be^{II} complexes[14] as it successfully recovered experimental stability trend; (i) the electronic structure calculations were performed with the 6-311++G(d,p) basis set modelled with implicit solvation (PCM/UFF) and water as the solvent and (ii) selected wavefunctions were submitted for QTAIM-defined[22] topological properties analysis and for the determination of IQA-defined properties using the AIMAll package.[23] As demonstrated recently,[14,24,25] the present limitations of AIMAll have no significant bearing on relative trends in the IQA-energy terms obtained at the DFT level even though an accurate implementation of IQA requires well-defined second order density matrix. Approximations used in AIMAll software result in a systematic error in the IQA-recovered molecular energy, the origin of which is mainly in the computed self-atomic energies. However, systematic error cancellation took place during a comparative analysis performed in this study. Our focus here is on relative trends rather than predicting energy terms on an absolute scale. Hence, the qualitative results and the conclusions arrived at from this work should be considered as valid. Non-Covalent Interactions[26-29] (NCI) isosurfaces were determined using NCIPlot 2.0[27] and these isosurfaces were visualized using VMD 1.9.1.

3. Results and Discussion

A protocol based on the competition reaction, CRn, described for Be^{II} complexes[14] was used to validate the optimized structures and select the most economic and suitable level of theory for further computations (for convenience details are shown in PART S1 of the SI).

Table 1. Computed ΔE_{CRn}, for the competition reaction for zinc ion using the lowest energy conformers of the ligands, NTA and NTPA, and their Zn^{II} complexes.

Method	E(aq)/au[a]				ΔE_{CRn}[b]
	ZnNTPA	NTA	ZnNTA	NTPA	
PBE1PBE	–2787.7180	–738.2275	–2669.8990	–856.0522	–3.6
B3LYP	–2789.1318	–739.0440	–2671.1665	–857.0189	–6.0
X3LYP	–2788.6367	–738.7590	–2670.7357	–856.6684	–5.2

[a] Electronic energy obtained by performing a single point calculation on the MP2 structure in solvent (PCM/UFF) using the 6-311++G(d,p) basis set. [b] Values in kcal mol^{-1}.

The structures of ligands and complexes, for which ΔE_{CRn} has been computed (Table 1), are shown in PART S1, Figures S1-S2 in the SI. It is clear that SPCs worked well, as was the case with Be^{II} complexes, predicting the preferential formation of ZnNTA at each level of theory. To get some appreciation of significance of the ΔE_{CRn} values we decided to compare it with

experimentally available formation constants. To this effect, Eq. 1 was used because the equilibrium constant for such a competition reaction can be determined by the difference of the formation constants of the competing complexes, here $\log K_1^{CRn}$ of 5.15.

$$\text{ZnNTPA} + \text{NTA} \leftrightarrow \text{ZnNTA} + \text{NTPA} \quad K_1^{CRn} = \frac{[\text{ZnNTA}][\text{NTPA}]}{[\text{ZnNTPA}][\text{NTA}]} \tag{1}$$

This can be converted into the free energy of the competition reaction using the well-known relationship, $\Delta G = -RT\ln K$, and a conversion factor of 1.36 kcal mol^{-1}, which is equivalent to 1 log$K$ unit. In this instance, $\Delta G_{CRn} = -7.0$ kcal mol^{-1} and it compares well with the ΔE_{CRn} values. It is important to realize that ΔE_{CRn} of about –5 to – 6 kcal mol^{-1} can be regarded as rather small relative to energies of complexes (–1.75 million kcal mol^{-1} for ZnNTPA and –1.68 million kcal mol^{-1} for ZnNTA), but it translates to a large difference in stability of complexes. This is because the experimentally obtained $\log K_1^{CRn}$ of about 5 implies that K_1 for ZnNTA is 10^5 times larger; hence the competition reaction 1 will go virtually to completion, with an analytically undetectable equilibrium concentration of ZnNTPA.

The computed ΔE_{CRn} values gave us the confidence to explore the full array of IQA/IQF-defined energetic properties at X3LYP as it accounts for weak intramolecular interactions somewhat better than B3LYP.[30-33] One must also recall that electronic energies can only be used by IQA/IQF energy partitioning schemes.

3.1. Relative Stability from Classical and IQA Indices

As also found in our previous work,[14] an extensive investigation of the plethora of local geometric and topological indices in the final molecular products has not provided a consistent picture which would allow to rationalize relative molecular stability (selected findings are included in PART S2 of the SI). Here, we analyse coordination bonds and steric clashes using the IQA-defined diatomic interaction. To distinguish between the different O-atoms, O(b)/O(nb) will represent a carboxylic O-atom in the ligand which is bonded/non-bonded to the Zn^{II} centre and O(w) will be used to represent the donor O-atom in water molecules. Lastly, we want to stress that all values reported in the Section 3.1 were computed without partitioning the complexes, *i.e.*, on the entirety of the $[Zn^{II}NTA(H_2O)_2]^-$ and $[Zn^{II}NTPA(H_2O)_2]^-$ molecules.

3.1.1. Strength of Coordination Bonds

It is important to investigate the strength of coordination bonds because, from an orthodox perspective, complex formation is an event between the metal centre and the donor atoms of a

ligand. It is also intuitive to link the strength of coordination bonds with determined relative stability of metal complexes. IQA-defined diatomic interaction energies, $E_{\text{int}}^{\text{Zn,X}}$, between the central metal ion and the donor atoms X are shown in Table 2.

All coordination bonds showed some mixed (covalent and ionic) character based on the $|V(r)|/G(r)$ ratio with the Zn–N bond in both complexes showing the most significant covalent contribution (PART S1,Table S1 in the SI); this appears to be a common feature of NTPA and NTA complexes.[13]

Table 2. The interatomic distances, d(Zn,X), IQA-interaction energies, $E_{\text{int}}^{\text{Zn,X}}$ and exchange-correlation component $V_{\text{XC}}^{\text{X,Y}}$, for the coordination bonds in ZnNTA and ZnNTPA at the X3LYP level of theory on the MP2 optimized structures.[a]

Bond	d(Zn,X)	$V_{\text{XC}}^{\text{X,Y}}$	$E_{\text{int}}^{\text{Zn,X}}$	Bond	d(Zn,X)	$V_{\text{XC}}^{\text{X,Y}}$	$E_{\text{int}}^{\text{Zn,X}}$
	ZnNTA				ZnNTPA		
Zn–N	2.130	–46.3	–273.2	Zn–N	2.127	–50.9	–272.0
Zn–O13(b)	2.060	–48.8	–300.2	Zn–O22(b)	2.019	–52.5	–311.1
Zn–O15(b)	2.058	–48.6	–300.8	Zn–O25(b)	2.029	–50.2	–306.8
Zn–O19(b)	2.057	–48.3	–301.9	Zn–O28(b)	2.037	–50.9	–307.9
	Sum:		**–1176.1**		**Sum:**		**–1197.8**
Zn–O21(w1)	2.222	–29.9	–250.2	Zn–O30(w1)	2.356	–20.0	–229.7
Zn–O22(w2)	2.139	–37.4	–268.3	Zn–O31(w2)	2.242	–28.7	–255.4
	Sum:		**–518.5**		**Sum:**		**–485.1**
	Total:		**–1694.6**		***Total:***		**–1682.9**

[a] d(Zn,X) is in Å; $E_{\text{int}}^{\text{Zn,X}}$ and $V_{\text{XC}}^{\text{X,Y}}$ are in kcal mol^{-1}.

Considering the interaction energies, the $E_{\text{int}}^{\text{Zn,N}}$ values in both complexes are comparable, but $E_{\text{int}}^{\text{Zn–O(b)}}$ are consistently more negative in ZnNTPA. As a result, the sum of the interaction energies is –1176.1 and –1197.8 kcal mol^{-1} in ZnNTA and ZnNTPA, respectively. This is an important finding as it demonstrates that 'affinity' of Zn^{II} to NTPA is significantly greater than to NTA; one must realize that here 'affinity' is expressed in terms of the coordination bond strengths. Hence, if one were to limit themselves to the coordination bonds (Zn–N and Zn–O^{-}) between the metal cation and ligand of interest, then ZnNTPA would be predicted as the preferentially formed complex, a clear contradiction of the experimental trend.

A different picture emerges when the interaction energies between Zn^{II} and O(w)-atoms are considered. Importantly, their sum is far more stabilizing in ZnNTA, as we found –518.5 and –485.1 kcal mol^{-1} in ZnNTA and ZnNTPA, respectively, and the total of these two contributions

favours ZnNTA by ~–12 kcal mol^{-1}, which correlates well with the experimental trend. This finding is of paramount importance as it strongly points at the coordinated water molecules as having an important (if not decisive) contribution to the relative stability of these complexes.

3.1.2. Origin of Strain in the Coordination Sphere.

The geometric (d(X,Y) < (the sum of the van der Waals (vdW) radii)) and IQA ($V_{XC}^{X,Y}$, $E_{int}^{X,Y}$) data for heteroatoms in the ZnNTA and ZnNTPA complexes is shown in Table 3. This is because it was suggested from MM calculations that such short internuclear contacts are among main contributors to strain.[1] To this effect, extensively commented NCI-based identification of strained regions in the coordination sphere is included in PART S2 of the SI.

Table 3. Geometric and IQA properties (diatomic interaction energy $E_{int}^{X,Y}$ and its component, $V_{XC}^{X,Y}$, obtained for repulsive interactions in the coordination spheres of ZnNTA and ZnNTPA at the X3LYP[a] level of theory on the MP2 optimized structure. Only data for atoms with the interatomic distance d(X,Y) < (sum of van der Waals radii) is included.

Interaction (X•••Y)	d(X,Y)	$V_{XC}^{X,Y}$	$E_{int}^{X,Y}$	Interaction (X•••Y)	d(X,Y)	$V_{XC}^{X,Y}$	$E_{int}^{X,Y}$
ZnNTA				ZnNTPA			
N•••O13(b)	2.709	–6.2	148.9	N•••O22(b)	3.087	–2.6	130.4
N•••O15(b)	2.772	–5.2	147.5	N•••O25(b)	3.016	–3.4	133.6
N•••O19(b)	2.812	–4.2	146.1	N•••O28(b)	3.050	–3.1	133.0
O19(b)•••O15(b)	3.001	–4.5	155.3	O30(w)•••O22(b)	2.667	–9.2	154.2
O21(w)•••O13(b)	2.886	–5.6	147.3	O30(w)•••O25(b)	2.881	–5.9	148.8
O21(w)•••O15(b)	2.823	–6.7	149.5	O31(w)•••O25(b)	2.749	–7.6	153.7
O22(w)•••O19(b)	2.813	–6.1	148.4	O31(w)•••O28(b)	2.820	–6.8	152.1
		Sum:	**1043.0**			**Sum:**	**1005.8**

[a] d(X,Y) is in Å; $E_{int}^{X,Y}$ and $V_{XC}^{X,Y}$ are in kcal mol^{-1}.

Classically, complex stability has been associated with the repulsion between lone-pair donor atoms coordinating to the central metal cation. As such, we have fully recovered this notion through highly positive, hence repulsive $E_{int}^{X,Y}$ values (X,Y = donor atoms O,N) which are about half in value of those between Zn^{II} and donor atoms of NTA and NTPA. Moreover, the O•••O interactions are more repulsive than O•••N interactions and particularly so in ZnNTPA. Note also that the N•••O interactions are significantly more repulsive in ZnNTA and this might be attributed to interatomic distances, d(N,O), which are between 0.25-0.35 Å shorter than in ZnNTPA.

As shown in Table 3, summed interaction energies produced +1043 kcal mol^{-1} for ZnNTA, which is about 37 kcal mol^{-1} larger when compared with ZnNTPA. The computed difference in repulsive intra-coordination sphere interactions is somewhat surprising as it goes against commonly accepted view that 6-memberd chelating rings (6m-CRs), such as in ZnNTPA, are highly strained relative to the 5m-CRs. We decided to expand our analysis by incorporating diatomic interaction energies between all donor-atoms of $\mathcal{L}$ and water molecules – PART S2,Table S5 in the SI. We found that:

- The sum of all interaction energies between donor atoms of the ligands is 861.6 and 818.1 kcal mol^{-1} in ZnNTA and ZnNTPA, respectively, hence larger in ZnNTA by 43.5 kcal mol^{-1} but summed interaction energies between donor atoms of a ligand (either NTA or NTPA) and O-atoms of water molecules is smaller in ZnNTA by 24 kcal mol^{-1} (1022.3 and 1046.0 kcal mol^{-1} in ZnNTA and ZnNTPA, respectively)
- The total destabilizing contribution made by repulsive interactions between donor atoms is +2019.3 and +1994.9 kcal mol^{-1} for ZnNTA and ZnNTPA, respectively.

Accounting for the contributions coming from all coordination bonds, including water molecules, we obtained –1694.7 and –1682.9 kcal mol^{-1} for ZnNTA and ZnNTPA, respectively; hence, the total energy contribution made by the coordination bonds is more stabilizing in ZnNTA by ~–12 kcal mol^{-1}. This, however, is not sufficient to either override the overwhelming number of repulsive interactions between donor atoms or shift the preference in favour of ZnNTA formation. The sum of all these diatomic interactions *in the coordinating region* amounts to a staggering +324.6 and +312.0 kcal mol^{-1} for ZnNTA and ZnNTPA, respectively. From that follows that there must be other significant and stabilizing in nature contributions; otherwise, these complexes would not form. Whilst summing the interaction energies in the coordination sphere worked well in the instance of Be^{II} complexes in identifying the preferentially formed BeNTPA complex, this is not the case of Zn^{II} complexes. The reason for that is simple if one recalls that Be^{II} complexes do not have coordinated water molecules.

The above analysis provided an invaluable insight (on a fundamental level) on properties in the coordination sphere but it failed entirely to explain experimental trend in log K_1 values.

3.1.3 Steric Contacts

Bader-defined molecular graphs[22] of the lowest energy conformers of ZnNTA and ZnNTPA are shown in Figure 2 where (i) a solid line linking two atoms represents diatomic interaction, which is commonly interpreted by chemists as a chemical bond, either covalent or coordination

bond in this case, and (ii) a dashed line reveals weaker interaction that fundamentally, in terms of density distribution between two atoms, does not differ from those ascribed to chemical bonds. Bader named these atomic interaction lines (AIL) bond paths (BPs) and made it absolutely clear that they must not be confused with a fussy concept of a chemical bond.[34] Recently, Foroutan-Nejad et al.[35] proposed to change nomenclature introduced by Bader by renaming a 'bond path' to a 'line path' in order to avoid 'interpretative' problems. Time will show whether this proposal will be widely accepted. In this work, however, we decided to use the original name, the 'atomic interaction line', because of two reasons, namely (i) in the IQA molecular energy partitioning scheme each atom interacts with any other in a molecular system (similar applies to IQF where each molecular fragment interacts with another) and the π-FARMS method is making use of the IQA/IQF concepts, and (ii) AIL points at its origin, hence gives full credit to Bader who developed QTAIM.[22]

For decades, based on geometric analyses and MM calculations, it has been advocated that steric –CH--HC– contacts are destabilizing any molecule including metal complexes.[1] Furthermore, these interactions were seen as a major source of strain in the coordinated ligands. This was also strongly supported by LFERs, which clearly showed good correlation between complexes forming 5m-CRs and 6m-CRs and experimentally available formation constants.

It was then of fundamental significance to investigate the nature, strength and significance of numerous (de)stabilizing intramolecular interactions. They were selected using interatomic distance smaller than the sum of the vdW radii (Table 4); a full set of topological properties at critical points (CPs) of atomic interaction lines (AILs) representing specific weak intramolecular interactions in ZnNTPA is shown in PART S2, Tables S3 in the SI.

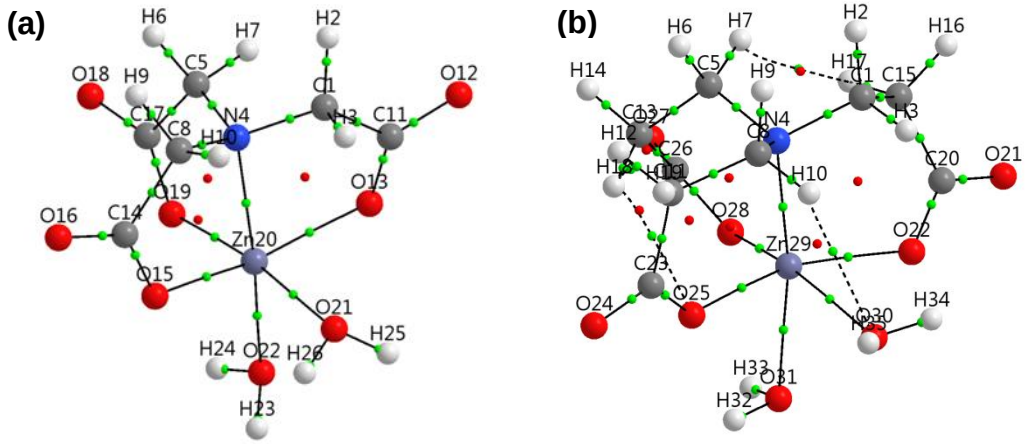

Figure 2. The QTAIM molecular graphs of the lowest energy conformers of (a) ZnNTA and (b) ZnNTPA.

Table 4. IQA partitioning of two-bodied interaction energies in ZnNTA and ZnNTPA for interactions of interest (the XL3YP wavefunction on the MP2 structures was used). In addition, geometric, selected topological and NCI isosurfaces are also included.

Interaction (X•••Y)	d(X,Y) Å	$\rho(r)$ au	NCI	q^{X} / e	q^{Y} / e	kcal mol^{-1}		
						$V_{cl}^{X,Y}$	$V_{XC}^{X,Y}$	$E_{int}^{X,Y}$
ZnNTA								
H2•••H7	2.378	no BP	Red	+0.0300	+0.0441	0.31	–0.82	–0.51
H6•••H9	2.160	no BP	Red	+0.0352	+0.0333	0.32	–2.16	–1.84
H3•••H10	2.123	no BP	Red	+0.0455	+0.0455	0.40	–2.16	–1.76
							Total:	**–4.1**
ZnNTPA								
H2•••H7	2.371	no BP	Red	+0.0100	+0.0223	0.14	–0.80	–0.66
H6•••H9	2.295	no BP	Red	+0.0191	+0.0085	0.17	–1.37	–1.19
H2•••H9	2.396	no BP	None	+0.0100	+0.0085	0.19	–1.17	–0.98
H3•••H10	2.207	no BP	Red	+0.0253	+0.0222	0.22	–1.71	–1.49
H6•••H12	2.255	no BP	Blue	+0.0191	+0.0236	0.09	–1.64	–1.55
H7•••H17	2.031	0.0134	Blue	+0.0223	+0.0251	0.08	–3.19	–3.11
H12•••H18	2.274	0.0092	Blue	+0.0236	+0.0248	0.06	–1.56	–1.50
							Sub-total:	**–10.5**
CH10•••O30(w1)	2.673	0.0078	Blue	+0.0222	–1.1516	–1.5	–3.3	–4.8
CH18•••O25(b)	2.563	0.0096	Blue	+0.0248	–1.2289	–2.5	–3.6	–6.1
OH32•••O25(b)	2.274	no BP	Blue	+0.6010	–1.2289	–101.0	–3.2	–104.1
OH34•••O22(b)	2.355	no BP	Blue	+0.5971	–1.2227	–98.9	–2.0	–100.8
OH35•••O25(b)	3.110	no BP	None	+0.5881	–1.2289	–78.5	–0.1	–78.6
							Total:	**–304.9**

Data shown in Table 4 can be used as a textbook example illustrating how analysis of individual indices, such as d(X,Y), $\rho(r)$ at CPs, presence/absence of AILs or NCI isosurfaces, might lead to incorrect and indeed contradictory conclusions.[36] To support this, let us point at some examples:

a) There is no correlation between interatomic distance, the exchange-correlation term, $V_{XC}^{X,Y}$, and the NCI-coloured isosurfaces. Red/blue isosurface is commonly attributed to repulsive/attractive interaction but we found red isosurface for H2•••H7 with d = 2.378 Å in ZnNTA whereas the H6•••H12 interaction in ZnNTPA is NCI-attractive (blue isosurface) even though interatomic distance is much shorter, by about 0.12 Å. All three H•••H interactions in ZnNTA show red NCI isosurfaces even though the first has very small XC-term, –0.8 kcal mol^{-1}, but the other two have XC-term nearly 3-times larger. H3•••H10 and H6•••H12 in ZnNTPA have red and blue, respectively, NCI isosurfaces even though the XC-term of –1.71 and –1.64 kcal mol^{-1}, respectively, and d(H,H) of 2.207 and 2.255 Å, respectively, are comparable.

b) Classical interatomic distance criterion does not correlate with absence/presence of AIL and this applies to many interactions in ZnNTPA. We found H12•••H18 with AIL and d = 2.274 Å whereas H3•••H10 with no AIL and shorter d = 2.207 Å. On the other hand, in the case of the H•••O interactions, CH18•••O25(b) with d = 2.563 Å has an AIL whereas a classical intramolecular H-bond with much shorter interatomic distance of 2.274 Å, OH32•••O25(b), does not have an AIL.

c) There is no correlation between strength of an interaction and presence/absence of an AIL. The OH32•••O25(b) interaction without AIL is highly stabilizing with $E_{\text{int}}^{\text{H32O25(b)}}$ = –104 kcal mol^{-1}, but CH18•••O25(b) with AIL has much smaller, $E_{\text{int}}^{\text{H18O25(b)}}$ of –6 kcal mol^{-1}. The differences in the interaction energy between the H- and O-atoms can be rationalized by the local environment. H18 is bonded to a less electronegative carbon atom whereas H32 is bonded to the highly electronegative oxygen atom. The charge on the H32-atom is significantly more positive than that on H18 (q^{H18} = +0.025 e and q^{H32} = +0.601 e) resulting in a larger difference in charge between the interacting atoms. This significantly increases the attractive $V_{\text{ne}}^{\text{H,O}}$ term and reduces the repulsive $V_{\text{ee}}^{\text{H,O}}$ term for the OH32•••O25(b) in ZnNTPA such that the overall classical term is 40 times more attractive relative to that found for CH18•••O25(b).

d) In general, all H•••O interactions have both attractive classical and XC terms, regardless of the presence/absence of an AIL or the presence/absence of an NCI-isosurface.

e) All CH•••HC interactions have small and comparable classical contributions regardless of (i) the interatomic distance, which varies between 2.031 and 2.396 Å, and (ii) the overall strength of the interaction energy $E_{\text{int}}^{\text{H,H}}$, which varies between +0.2 and –3.1 kcal mol^{-1}. Note that the red isosurfaces can only be found between αH-atoms for which the XC-term varies between –0.8 and –2.2 kcal mol^{-1} and according to NCI-based common interpretations, these atoms are strained in both complexes. However, all three NCI-strained CH•••HC interactions in ZnNTA contribute in stabilizing nature when one considers the IQA-defined $E_{\text{int}}^{\text{H,H}}$ term, in total –4.1 kcal mol^{-1}. Furthermore, the CH•••HC interactions in ZnNTPA contribute –10.5 kcal mol^{-1}, which is over twice as much as found in ZnNTA which is in direct conflict with classical views.

In general, the only consistent description of the CH•••HC interactions we obtained from the analysis of the IQA defined energy terms. One of the reviewers suggested that it would be of interest to examine previously suggested link between the IQA-defined XC-term ($V_{\text{XC}}^{\text{X,Y}}$) and

QTAIM-defined delocalization index (*DI*) using our molecular systems. This is because validity of such relationship has been explored for limited number of molecular systems.[37-40]

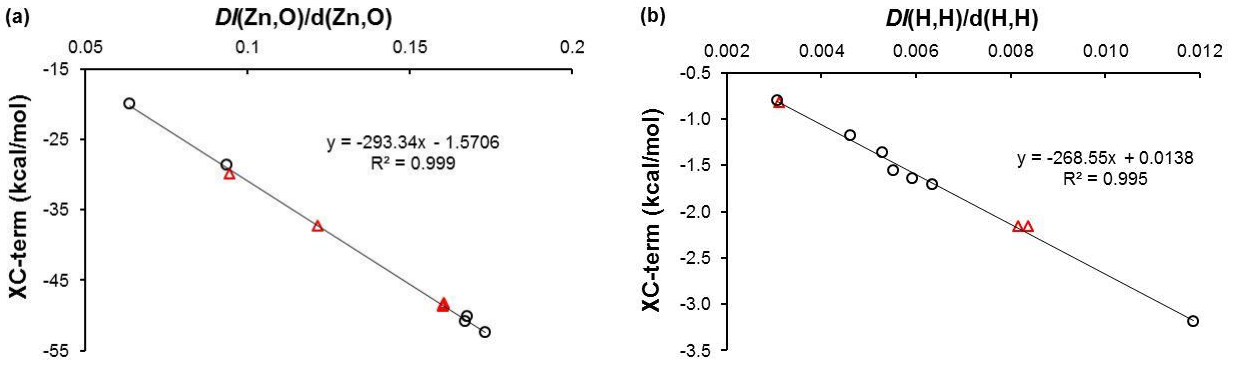

Figure 3. Relationships between the XC-term and normalized by interatomic distance delocalization index, *DI*(X,Y)/d(X,Y), for (a) -coordination Zn–O bonds and (b) - intramolecular H•••H interactions. Data obtained for ZnNTA and ZnNTPA complexes are represented by circles and triangles, respectively. Trend lines were fitted for the combined data coming from two complexes.

Nearly perfect linear relationships between the XC-term and normalized by interatomic distance delocalization index were obtained for coordination bonds between the central metal ion Zn^{II} and O-donor atoms as well as H•••H intramolecular interactions - see part (a) and (b), respectively, in Figure 3. Data shown in Figure 3 is of fundamental significance as it nicely illustrates how electron density is distributed between any two atoms in a molecular system. Recall that in the IQA energy partitioning scheme there are only two energy components, self-atomic and diatomic interaction energy, used to recover the electronic energy of a molecular system. Moreover, all atoms are treated on equal footing regardless whether they are bonded, as perceived by classical chemists, or not. From this follows that there is always some XC-component attributed to a specific pair of atoms regardless how close or far away they are and this appears to correlate very well with the QTAIM-defined delocalization index, *DI*(X,Y). Note that very much the same quality relationships were obtained for combined from both complexes coordination Zn–O bonds and H•••H intramolecular interactions, regardless whether AIL was present or absent in the latter case. Our results, in combination with earlier reports,[37-40] strongly suggest that the relationships shown in Figure 3 are universal provided, in our opinion, that they are generated for a specific interaction (pair of atoms) in similar molecular environment.

Unfortunately, none of the above can be used to explain relative stability of molecular systems. Hence, we decided to change the focus from interpreting isolated geometric and physical properties to understanding processes involved in complex formation.

3.2. Application of the π-FARMS Method on Zn^{II} Complexes

The π-FARMS methodology, introduced in the work on Be^{II} complexes,[14] makes use of numerous IQA/IQF-defined energy terms to explore changes taking place in selected molecular fragments from which the origin of relative stability of compounds can be deduced on a fundamental level. To achieve that, we consider the formation of a molecular system as made of two simple, yet intuitive stages, which are shown in Scheme 1 for 2-fragment partitioning scheme:

Scheme 1. Two-step decomposition of the complex formation process.

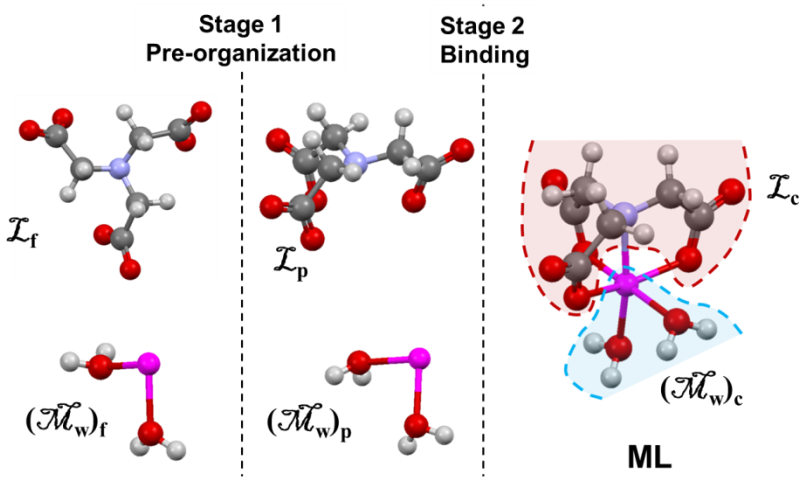

a) Stage 1 represents the preorganization from a "free" fragment ($\mathcal{I}_f$ or $(\mathcal{M}_w)_f$) to that as observed in the complex ($\mathcal{I}_p$ or $(\mathcal{M}_w)_p$). By decomposing a preorganization energies, that of a ligand $E^{\mathcal{I}}_{p-org}$ and of a metal-containing fragment $E^{\mathcal{M}_w}_{p-org}$, we will attempt to discover the origin of strain.

b) Stage 2 represents the reaction between preorganized fragments $\mathcal{I}_p$ and $(\mathcal{M}_w)_p$ to form a complex ML; the energy released can be seen as the binding energy, E^{ML}_{bind}. We will also explore here the fundamental changes occurring within molecular fragments when $\mathcal{I}_p$ and $(\mathcal{M}_w)_p$ become parts of a complex ML, $\mathcal{I}_c$ and $(\mathcal{M}_w)_c$, because the atomic and interatomic properties are completely different due to the presence of additional interactions.

3.2.1. An initial insight from pre-organization and binding electronic energies

The preorganization energies related to the first stage in Scheme 1 can be computed from Eq. 2 for a ligand and Eq. 3 for a metal containing fragment,

$$E^{\mathcal{L}}_{\text{p–org}} = E(\mathcal{L}_{\text{p}}) - E(\mathcal{L}_{\text{f}}) \quad (2)$$

$$E^{\mathcal{M}_{\text{w}}}_{\text{p–org}} = E((\mathcal{M}_{\text{w}})_{\text{p}}) - E((\mathcal{M}_{\text{w}})_{\text{f}}). \quad (3)$$

The binding energy between the pre-organized fragments in Stage 2 can be expressed as

$$E^{\text{ML}}_{\text{bind}} = E(\text{ML}) - E(\mathcal{L}_{\text{p}}) - E((\mathcal{M}_{\text{w}})_{\text{p}}). \quad (4)$$

The energetic sum of these two processes, $E^{\mathcal{L}}_{\text{p–org}} + E^{\mathcal{M}_{\text{w}}}_{\text{p–org}} + E^{\text{ML}}_{\text{bind}}$, amounts to the resultant energy change on complex formation, $\Delta E_{\text{ML}} = E(\text{ML}) - E(\mathcal{L}_{\text{f}}) - E((\mathcal{M}_{\text{w}})_{\text{f}})$, related to the reaction of the free metal fragment $(\mathcal{M}_{\text{w}})_{\text{f}}$ with the free ligand $\mathcal{L}_{\text{f}}$. The usefulness of this approach is that it combines all energy contributions into predefined and meaningful terms, which agree with a chemists' intuition. It is also a first and necessary step in the π-FARMS methodology as these energy terms can be used for partitioning in the IQA/IQF-based analysis.

Data in Table 5 shows that both ligands became strained because their energy increased when they changed from $\mathcal{L}_{\text{f}}$ to $\mathcal{L}_{\text{p}}$ structure. This process incurred greater strain in NTPA, $E^{\text{NTPA}}_{\text{p–org}} > E^{\text{NTA}}_{\text{p–org}}$, by about 11.5 kcal mol^{-1} at X3LYP; the same trend was also found for the Ni^{II} and Be^{II} complexes. Regardless of complex formed, a lesser preorganization energy is always found for the metal-containing fragments. Moreover, the $(\mathcal{M}_{\text{w}})_{\text{p}}$ fragment binding to NTPA acquired greater strain and we obtained $E^{\mathcal{M}_{\text{w}}}_{\text{p–org}}(\text{ZnNTPA}) - E^{\mathcal{M}_{\text{w}}}_{\text{p–org}}(\text{ZnNTA})$ of about 6.1 kcal mol^{-1}. Zn^{II} forms complexes with NTA and NTPA spontaneously. From this it follows that for both complexes

Table 5. Computed preorganization (strain) energies and binding energies (all in kcal mol^{-1}) using relevant energy terms obtained for $(\mathcal{M}_{\text{w}})_{\text{f}}$, $\mathcal{L}_{\text{f}}$ of NTA and NTPA, the complexes ZnNTA and ZnNTPA, and the respective $(\mathcal{M}_{\text{w}})_{\text{p}}$ and $\mathcal{L}_{\text{p}}$ at the X3LYP level of theory on the MP2 optimized structures.

$E^{\mathcal{M}_{\text{w}}}_{\text{p–org}}$			$E^{\mathcal{L}}_{\text{p–org}}$			$E^{\text{ML}}_{\text{bind}}$			ΔE_{ML} [a]
NTA	NTPA	$\Delta E^{\mathcal{M}_{\text{w}}}_{\text{p–org}}$ [b]	NTA	NTPA	$\Delta E^{\mathcal{L}}_{\text{p–org}}$ [c]	ZnNTA	ZnNTPA	$\Delta E^{\text{ML}}_{\text{bind}}$ [d]	
2.8	8.8	6.1	19.5	31.1	11.5	–104.5	–116.9	–12.4	5.2

[a] $\Delta E_{\text{ML}} = E_{\text{ZnNTPA}} - E_{\text{ZnNTA}}$; [b] $\Delta E^{\mathcal{M}_{\text{w}}}_{\text{p–org}} = E^{\mathcal{M}_{\text{w}}}_{\text{p–org}}(\text{ZnNTPA}) - E^{\mathcal{M}_{\text{w}}}_{\text{p–org}}(\text{ZnNTA})$; [c] $\Delta E^{\mathcal{L}}_{\text{p-org}} = E^{\text{NTPA}}_{\text{p-org}} - E^{\text{NTA}}_{\text{p-org}}$;
[d] $\Delta E^{\text{ML}}_{\text{bind}} = E^{\text{ZnNTPA}}_{\text{bind}} - E^{\text{ZnNTA}}_{\text{bind}}$.

the binding energy between ligand and the metal-containing fragment must override strain incurred during the preorganization of both fragments; this is exactly recovered from our computations. Moreover, we found that affinity of Zn^{II} to NTPA (as measured now by the binding energy) is more favourable with $\Delta E^{\text{ML}}_{\text{bind}} \sim -12.4$ kcal mol^{-1}. This is consistent with the

computed strengths of coordination bonds with $\mathcal{L}$; $\Delta E_{\text{int}}^{\text{Zn,X}}$ = ~–22 kcal mol^{-1} in favour of ZnNTPA (Table 2). We can also make another important observation of fundamental significance, namely that preorganization and binding energies of $\mathcal{L}$ cannot explain preferential formation of ZnNTA. This is because $\Delta E_{\text{p–org}}^{\mathcal{L}} + \Delta E_{\text{bind}}$ = – 0.9 kcal mol^{-1} is in favour of ZnNTPA. This finding clearly demonstrates that this is not the structural property of a ligand or the nature of the CH--HC contacts (main focus of previous studies[13]) but the preorganization energy of the metal-containing fragment, $E_{\text{p–org}}^{\mathcal{M}_{\text{w}}}$, that plays a significant and determining role in the relative stability of these metal complexes. Interestingly, we arrived at the same conclusion from the analysis of coordination bond strengths in 3.1.1. Section.

The validity of this protocol comes from the ability to fully recover the experimental trend. The relative difference in the complex formation energy is given by

$$\Delta E_{\text{ML}} = (E_{\text{p–org}}^{\text{NTPA}} + E_{\text{p–org}}^{\mathcal{M}_{\text{w}}}(\text{ZnNTPA}) + E_{\text{bind}}^{\text{ZnNTPA}}) - (E_{\text{p–org}}^{\text{NTA}} + E_{\text{p–org}}^{\mathcal{M}_{\text{w}}}(\text{ZnNTA}) + E_{\text{bind}}^{\text{ZnNTA}}) \qquad (5)$$

and, at the X3LYP level of theory, we obtained ΔE_{ML} of 5.2 kcal mol^{-1} not in favour of ZnNTPA, corresponding to the experimental trend. Moreover, this fully recovers E_{CRn}, as $\Delta E_{\text{CRn}} = -\Delta E_{\text{ML}}$, further reinforcing the validity of the protocol.

It is important to stress that this is not the first attempt at understanding relative molecular stability using an *energetic* decomposition of the formation energy. An energy decomposition scheme, ETS-NOCV,[7-9] was used in the previous study of Zn^{II} complexes of NTA and NTPA;[13] Table 6 summarizes the results obtained. The distortion energy of each fragment, ΔE_{dist}, is the ETS-NOCV term equivalent to the preorganization energy of the fragment, $E_{\text{p-org}}$, and the interaction energy, ΔE_{int}, corresponds to the binding energy, E_{bind}. As one would expect, ETS-NOCV and relevant energy terms computed here differ in values, as they should, but the most striking observation is the fact that all conclusions we arrived at above one can fully recover from the data in Table 6, namely:

a) Zn^{II} has higher affinity to NTPA because $\Delta\Delta E_{\text{int}}$ is negative, –23.4 kcal mol^{-1}.
b) Larger energy penalties are required to pre-organise the free ligand and water-containing metal fragment for the ZnNTPA formation, the relevant ΔE_{dist} terms.
c) Combining differences in interaction and ligand distortion energies cannot explain preferential formation of ZnNTPA because $\Delta\Delta E_{\text{int}}$ = –23.4 kcal mol^{-1}+ $\Delta\Delta E_{\text{dist-}\mathcal{L}}$ = +11.3 kcal mol^{-1} < 0, hence in favour of ZnNTPA again.

d) Coordinated water molecules play an important role in controlling relative stability of metal complexes as the $\{\Delta E_{\text{total}}\}_{\text{ZnNTA}}$ value is more negative than $\{\Delta E_{\text{total}}\}_{\text{ZnNTPA}}$; hence, it is in favour of ZnNTA in accord with experimental data.

Table 6. ETS-NOCV results[13] describing energy contributions making up energy[a] of complex formation. All values in kcal mol^{-1}.

Energy term	ZnNTA	ZnNTPA	ΔE^{b}
ETS-NOCV Energy components related to $E_{\text{p-org}}$			
$\Delta E_{\text{dist-}\mathcal{M}}$	21.1	37.3	16.2
$\Delta E_{\text{dist-}\mathcal{L}}$	20.5	31.8	11.3
ΔE_{dist}	41.6	69.1	27.6
ETS-NOCV Energy components related to $E_{\text{bind}}^{\text{ML}}$			
ΔE_{int}	–148.7	–172.1	–23.4
ETS-NOCV Energy components related to ΔE_{ML}			
$\Delta E_{\text{total (solvent)}}$	–107.1	–103.0	4.1

[a] The Becke-Perdew exchange correlation functional (BP86) was applied with the standard double-ζ STO basis set on all atoms except Zn, where the TZP basis set was employed. This was done in the COSMO solvation model using water as solvent. [b] $\Delta E = E(\text{NTPA}) - E(\text{NTA})$

3.2.2. The pre-organization energy of a $\mathcal{L}_{\text{p}}$ from IQA perspective

An excellent agreement between data shown in Tables 5-6 is highly gratifying but says nothing about the origin of these results. For completeness, a detailed discussion of the QTAIM molecular graphs and NCI isosurfaces of pre-organized ligands, as found in ZnNTA and ZnNTPA complexes, is included in PART S3 of the SI. As one would anticipate, the interpretation of interactions revealed in $\mathcal{L}_{\text{p}}^{\text{NTA}}$ and $\mathcal{L}_{\text{p}}^{\text{NTPA}}$ is as inconsistent, uncertain and highly speculative as found for metal complexes in previous sections. Hence, to gain an insight on the energetic origin of strain in the ligands we decided to use IQA-defined intra- and interatomic properties.

The energy of a molecule, or any molecular fragment, is the sum of the additive energies, $E_{\text{add}}^{\text{X}}$, of each atom in the molecule,

$$E = \sum_{\text{X}} E_{\text{add}}^{\text{X}} \quad .. \tag{6}$$

Additionally, the additive energy of an atom is defined in IQA as,

$$E^{X}_{add} = E^{X}_{self} + \sum_{Y \neq X} 0.5 E^{X,Y}_{int} \quad (7)$$

where the first term is the intra-atomic contribution (self-atomic energy) and the second term is the interatomic contribution (sum of halved diatomic interaction energies). One can trace the changes in these three energy terms of all atoms when the ligand changes from the $\mathcal{I}_f$ to $\mathcal{I}_p$ structure. Table 7 shows such changes as $\Delta U^X = U_{p\text{-}org} - U_{free}$ for each atomic property U for a selected arm of each ligand. Naturally, the atoms with the most significant change in the additive energy, ΔE^X_{add}, have the greatest impact on the energy of the molecule. Thus, if an atom experiences a significant increase in the additive energy, then the atom is destabilized and contributes significantly to the overall strain of the molecule. Furthermore, Eq. 7 allows one to trace back the origin of strain, namely either to an atom itself or to unfavourable molecular environment when the interaction energy with remaining atoms of a molecular system has increased; the latter can be interpreted as intra-molecular/fragment strain. In paragraphs that follow we will restrain ourselves to the analysis of energy terms contributing to strain; detailed explanation and analysis of relevant physical properties is available in PART S3, Tables S6 in the SI.

Let us first analyse H-atoms in both ligands. We found that all three energy terms in Eq. 7 have changed an order(s) of magnitude less when compared with atoms of the carboxylate groups and the N-atoms. Thus, contrary to what is contemporary knowledge, H-atoms involved in a steric clash negligibly contribute to destabilizing the molecule; the largest ΔE^X_{add} = +1.4 kcal mol^{-1} was found for H12 in NTPA (PART S3, Table S6 in the SI), which is involved in an attractive interaction with H6 (–1.5 kcal mol^{-1}) without AIL but with density accumulated in the interatomic region – see Table 4.

Focussing on N-atoms and atoms of the carboxylate groups, the preorganization of the ligands resulted in more pronounced changes in NTPA and the following pattern emerges:

- The highly negatively charged atoms, N, O(b) and O(nb) (except N-atom in NTA), experienced a large increase in atomic additive energies. The main contribution comes from unfavourable molecular environment, resulting in $\sum_{Y \neq X} 0.5 E^{X,Y}_{int} >> 0$, in case of N and O(b), for which an outflow of electron density is observed, $\Delta N^X < 0$. Just the opposite was found for the O(nb) atoms in both ligands, $\sum_{Y \neq X} 0.5 E^{O(nb),Y}_{int} < 0$ and $\Delta N^{O(nb)} > 0$; note also that an increase in $E^{O(nb)}_{self}$ is more significant than change in interaction energy term.

- The highly positively charged γC-atoms of the carboxylate groups (i) found themselves in a more favourable environment and (ii) gained electron density, $\Delta N^{\gamma C} > 0$. This resulted in both contributions to additive energy (Eq 7) being of stabilizing nature and γC-atoms being stabilized the most among all atoms in both ligands.

In conclusion, we would like to stress that all these trends are identical to those found for the Be^{II} complexes,[14] suggesting that the changes in the ligand do not depend on the size of the metal ion coordinated or the size, 5m-CR or 6m-CR, of chelating ring. Furthermore, in relation to classical interpretations, our results:

- Confirm that the coordination spheres are strained.
- Confirm that NTPA is more strained and origin can be linked with far more repulsive interactions between coordinating atoms, O(b) and N.
- Contradict a classical notion of the highly repulsive and destabilizing nature of H-atoms involved in steric contacts.

3.2.3. The pre-organization energy of a $(\mathcal{M}_w)_p$ from IQA perspective

QTAIM molecular graphs or NCI isosurfaces shown no additional intra-fragment interactions in the $(\mathcal{M}_w)_p$ structures; hence, we traced the origin of preorganization energies from the IQA-perspectives – see Table 7 and extensively commented Table S7, PART S3 of the SI. The variations in all energy terms, when $(\mathcal{M}_w)_f$ changed to $(\mathcal{M}_w)_p$, shows that by far more significant changes took place in $(\mathcal{M}_w)_p^{NTPA}$. Furthermore, except H26 in $(\mathcal{M}_w)_p^{NTA}$ and H34 in $(\mathcal{M}_w)_p^{NTPA}$, changes in interaction energies are more significant than that found for self-atomic energies. However, regardless of the magnitude of changes, there appears to be a consistent pattern in both systems:

- The largest destabilizing contribution to the energy of $(\mathcal{M}_w)_p$ came from Zn^{II} in both fragments. Preorganization of the fragment resulted in (i) the dissipation of electron density from Zn^{II} into the surrounding environment, $\Delta N^{Zn} < 0$, and (ii) largest increase in the additive atomic energy of Zn^{II}, E_{add}^{Zn}.
- Considering equatorial water molecules of both $(\mathcal{M}_w)_p$ fragments: (i) H-atoms became stabilized by two energy components of their additive atomic energies, but (ii) O-atoms experienced highly unfavourable interaction term, which overcompensated a stabilizing and significant change in their self-atomic energies.

- Additive energies of all atoms of the axial water molecules have increased even though opposite trends in electron population are observed; we found that $\Delta N^{O} < 0$ whereas $\Delta N^{H} > 0$ and this, in combination with $\Delta N^{Zn} < 0$ shows that electron density was dissipated to H-atoms.

Table 7. Relative to $(\mathscr{M}_w)_f$ structures, changes in the selected IQA-defined energy terms (values in kcal mol^{-1} at the RX3LYP level of theory on the MP2 structure).

	$(\mathscr{M}_w)_p^{NTA}$				$(\mathscr{M}_w)_p^{NTPA}$		
Atom X	ΔE_{add}^{X}	$\sum_{Y\neq X} 0.5E_{int}^{X,Y}$	ΔE_{self}^{X}	Atom X	ΔE_{add}^{X}	$\sum_{Y\neq X} 0.5E_{int}^{X,Y}$	ΔE_{self}^{X}
Zn20	10.8	9.6	1.2	Zn29	28.4	20.8	7.6
Equatorial water molecules							
O21	0.6	9.7	–9.1	O30	7.6	22.8	–15.3
H25	–5.3	–3.3	–2.0	H34	–10.0	–4.2	–5.8
H26	–4.5	–1.8	–2.8	H35	–11.8	–8.6	–3.3
Axial water molecules							
O22	1.6	5.7	–4.1	O31	13.3	25.4	–12.0
H23	3.8	3.8	0.0	H32	0.6	4.4	–3.8
H24	3.7	5.2	–1.6	H33	0.5	3.8	–3.3

Interestingly, the same physical phenomenon (the outflow of electron density and the expansion of the atomic volume) resulted in the increase of the self-energy of the zinc centre but the decrease in self-atomic energies of the O-atoms. This is because the self-atomic energy of an atom is lowest in the isolated neutral state. An outflow of electron density from a positively charged atom (such as Zn^{2+}) results in a further deviation in density from the neutral Zn atom. On the other hand, an outflow of electron density from a negatively charged atom (such as O-atoms) is a movement towards the neutral ground state and hence the self-atomic energy decreases.

To gain deeper insight, the changes in all unique diatomic interaction energies within the metal-containing fragments were analysed – relevant data are included in Table S8, PART S3 of the SI. The origin of the greater penalty for pre-organizing $(\mathscr{M}_w)_p^{NTPA}$ can be attributed to specific interactions. In both metal complexes, the coordination Zn–O(w) bonds to equatorial water molecules show the greatest destabilization with $\Delta E_{int}^{Zn,O21}$ = +19.9 and $\Delta E_{int}^{Zn,O30}$ = +40.4 kcalmol^{-1} in $(\mathscr{M}_w)_p^{NTA}$ and $(\mathscr{M}_w)_p^{NTPA}$, respectively. The increases are a result of elongation of the coordination bonds when the metal-containing fragment changes from $(\mathscr{M}_w)_f$ to $(\mathscr{M}_w)_p$. The Zn–

O(w1) bond increases by 0.116 and 0.250 Å in $(\mathcal{M}_w)_p^{NTA}$ and $(\mathcal{M}_w)_p^{NTPA}$ respectively. Significantly smaller increases in coordination bonds are found for axial water molecules, by 0.034 and 0.137 Å, which is accompanied by less unfavourable changes in interaction energies, $\Delta E_{int}^{Zn,O22}$= +4.4 and $\Delta E_{int}^{Zn,O31}$= +18.7 kcal mol^{-1} in $(\mathcal{M}_w)_p^{NTA}$ and $(\mathcal{M}_w)_p^{NTPA}$, respectively.

Importantly, all the above trends correspond to properties of the coordination bonds in Table 2; the Zn–O(w) bond was found to be stronger in ZnNTA across all techniques, and showed the lesser deviations from the $(\mathcal{M}_w)_f$ structure during preorganization.

3.2.4. Binding between two pre-organized fragments from the IQF perspective

To gain an insight into the mechanism and energetic origin of the binding process, we decomposed E_{bind}^{ML} utilizing the IQF concepts; this resulted in a protocol applicable to any molecular system. The full derivation of terms used is shown in PART S4 of the SI. However, there are particular terms of interest, which we would like to turn our attention to. Firstly, within the IQF framework, the binding energy is the sum of the interaction energies between all fragments and the deformation energies of each individual fragment. In the instances of metal complexes, E_{bind}^{ML} is expressed as:

$$E_{bind}^{ML} = E_{def}^{\mathcal{M}_w} + E_{def}^{\mathcal{I}} + E_{int}^{(\mathcal{M}_w)_c,\mathcal{I}_c} \tag{8}$$

The deformation energy of each fragment can be partitioned to the contributions made due to change in (i) the self-energy of the fragment ($\Delta E_{self}^{\mathcal{M}_w}$ and $\Delta E_{self}^{\mathcal{I}}$) and (ii) the diatomic interaction energies within the fragment ($\Delta E_{int}^{\mathcal{M}_w}$ and $\Delta E_{int}^{\mathcal{I}}$) when they changed from pre-organized to that in the complex state. Thus the binding energy may be written as:

$$E_{bind}^{ML} = \Delta E_{self}^{\mathcal{M}_w} + \Delta E_{self}^{\mathcal{I}} + \Delta E_{int}^{\mathcal{M}_w} + \Delta E_{int}^{\mathcal{I}} + E_{int}^{(\mathcal{M}_w)_c,\mathcal{I}_c} \tag{9}$$

The interaction energy between two fragments is composed of the classical and the exchange-correlation components and is obtained by summing these contributions from all interactions between the fragments:

$$E_{int}^{(\mathcal{M}_w)_c,\mathcal{I}_c} = V_{cl}^{(\mathcal{M}_w)_c,\mathcal{I}_c} + V_{XC}^{(\mathcal{M}_w)_c,\mathcal{I}_c} = \sum_{X\in(\mathcal{M}_w)_c}\sum_{Y\in\mathcal{I}_c} V_{cl}^{X,Y} + \sum_{X\in(\mathcal{M}_w)_c}\sum_{Y\in\mathcal{I}_c} V_{XC}^{X,Y} \tag{10}$$

Table 8 shows the IQF-related energy terms used to evaluate the binding energy of the two complexes and it is clear that binding is highly stabilizing and in favour of ZnNTPA, $\Delta E_{\text{bind}}^{\text{ML}} = E_{\text{bind}}^{\text{ZnNTPA}} - E_{\text{bind}}^{\text{ZnNTA}} = -23.8$ kcal mol^{-1}. The binding is driven by the inter-fragment interaction

Table 8. The indicated energy components (in kcal mol^{-1}), computed within a IQF framework, which were used in the interpretation of relative stability of ZnNTA and ZnNTPA complexes when 2-fragment partitioning was used.

Energy term	ZnNTA	ZnNTPA	ΔE[a]
Energy components of E_{bind}			
$E_{\text{def}}^{\mathcal{M}_{\text{w}}}$	–101.8	–99.8	2.0
$E_{\text{def}}^{\mathcal{L}}$	56.3	87.1	30.8
$E_{\text{int}}^{(\mathcal{M}_{\text{w}})_{\text{c}},\mathcal{L}_{\text{c}}}$	–672.1	–728.9	–56.7
$E_{\text{bind}}^{\text{ML}}$	–717.6	–741.4	–23.8
Additional energy terms			
$\Delta E_{\text{self}}^{\text{ML}}$	30.2	72.7	42.5
$\Delta E_{\text{self}}^{\mathcal{M}_{\text{w}}}$	–108.5	–100.8	7.7
$\Delta E_{\text{int}}^{\mathcal{M}_{\text{w}}}$	6.7	1.0	–5.7
$\Delta E_{\text{self}}^{\mathcal{L}}$	138.7	173.4	34.7
$\Delta E_{\text{int}}^{\mathcal{L}}$	–82.4	–86.3	–3.8
$V_{\text{cl}}^{(\mathcal{M}_{\text{w}})_{\text{c}},\mathcal{L}_{\text{c}}}$	–443.4	–466.5	–23.1
$V_{\text{XC}}^{(\mathcal{M}_{\text{w}})_{\text{c}},\mathcal{L}_{\text{c}}}$	–228.7	–262.3	–33.6

[a] $\Delta E = E(\text{NTPA}) - E(\text{NTA})$

energy term, $E_{\text{int}}^{(\mathcal{M}_{\text{w}})_{\text{c}},\mathcal{L}_{\text{c}}}$; the affinity to the metal-containing fragment to a ligand is (i) highly attractive for both complexes and (ii) an order of magnitude larger than the deformation energy component. Recall that the sum of the interaction energies of the coordination bonds to the ligand predicted the preferential formation of ZnNTPA by ~21 kcal mol^{-1} and this result remarkably agrees with the trend in binding. For both complexes, the binding process clearly results in (i) the stabilization of metal-containing fragment, $E_{\text{def}}^{\mathcal{M}_{\text{w}}} < 0$, and the stabilization is marginally, by 2.0 kcal mol^{-1}, in favour of ZnNTA (ii) the positive deformation energy of the ligands, $E_{\text{def}}^{\mathcal{L}} > 0$, which is a far greater energy penalty in the case of NTPA, by ~31 kcal mol^{-1}. Note that the value of the inter-fragment interaction energy term between $(\mathcal{M}_{\text{w}})_{\text{c}}$ and $\mathcal{L}_{\text{c}}$, is significantly smaller than the sum of the interaction energies computed for coordination bonds.

This is an important finding as it reveals that there are additional interactions contributing unfavourably to the binding energy, as also found for Be^{II} complexes.[14]

In search for the origin of the fragments' deformation energies, we turn our attention to the additional terms, shown in Table 8. They reveal that the contribution of the fragments' self-energies results in the overall deformation energy, $\Delta E_{\text{self}}^{\text{ML}}$, being destabilizing in both complexes and much larger in ZnNTPA, by about 42.5 kcal mol^{-1}. The source of $\Delta E_{\text{self}}^{\text{ML}} > 0$ can be traced to the self-energy of a ligand fragment because $\Delta E_{\text{self}}^{\mathcal{L}}$ of +138.7/+173.4 kcal mol^{-1} in NTA/NTPA, respectively, is much larger than stabilizing in nature change in the metal-containing fragments' self-energies, $\Delta E_{\text{self}}^{\mathcal{M}_{\text{w}}}$ of –108.5/–100.8 kcal mol^{-1} in NTA/NTPA, respectively. Moreover, we found that the intra-fragment interaction energy is (i) stabilizing for the ligand fragments, $\Delta E_{\text{int}}^{\mathcal{L}} < 0$, (ii) destabilizing for both the Zn-containing fragments, $\Delta E_{\text{int}}^{\mathcal{M}_{\text{w}}} > 0$, (iii) in absolute values, $\Delta E_{\text{int}}^{\mathcal{L}} >> \Delta E_{\text{int}}^{\mathcal{M}_{\text{w}}}$, and (iv) both these energy components changed in favour of ZnNTPA by a few kcal mol^{-1} in both complexes.

Focusing on most significant in value the inter-fragment interaction energy, it is clear that this term is dominated by the electrostatic attraction between the fragments, $V_{\text{cl}}^{(\mathcal{M}_{\text{w}})_{\text{c}},\mathcal{L}_{\text{c}}}$, and it is –23.1 kcal mol^{-1} more attractive in ZnNTPA. Pendás *et al*[20] described the classical (electrostatic) term as being equivalent to the electrostatic term (ΔV_{elstat}) of EDA, which is also found in the ETS-NOCV scheme. Note that the trend $\left| V_{\text{cl}}^{(\mathcal{M}_{\text{w}})_{\text{c}},\mathcal{L}_{\text{c}}}(\text{ZnNTPA}) \right| > \left| V_{\text{cl}}^{(\mathcal{M}_{\text{w}})_{\text{c}},\mathcal{L}_{\text{c}}}(\text{ZnNTA}) \right|$ is the same as found for Zn^{II} complexes previously using ETS-NOCV.[13] Additionally, there is a significant exchange-correlation term $V_{\text{XC}}^{(\mathcal{M}_{\text{w}})_{\text{c}},\mathcal{L}_{\text{c}}}$ that is the same order of magnitude as the classical term. Note that both terms, classical and XC, are by far more stabilizing in ZnNTPA, by –33.6 and –23.1 kcal mol^{-1}, respectively.

3.2.5. Binding between four pre-organized fragments from the IQF perspective

The above decomposition identifies that the favourable binding of ZnNTPA is due to the more attractive interaction energy between $(\mathcal{M}_{\text{w}})_{\text{c}}$ and $\mathcal{L}_{\text{c}}$ but it is unclear which interactions are responsible. It is ineffective and time consuming to analyse every single interaction between the two fragments; there are 196 individual interactions for ZnNTPA and 133 in ZnNTA. To eliminate interactions that do not contribute significantly, the binding step was decomposed

alternatively; rather than using two fragments, four chemically sound fragments were used. The binding energy using a 4-component approach can be calculated as follows:

$$E_{\text{bind}}^{\text{ML}} = E(\text{ML}) - E(\mathcal{L}_{\text{p}}) - E(\mathcal{M}_{\text{f}}) - E((\mathcal{W}_1^{\text{o}})_{\text{p}}) - E((\mathcal{W}_2^{\text{o}})_{\text{p}}). \quad (11)$$

Using the electronic energy at the X3LYP level of theory, we found $E_{\text{bind}}^{\text{ZnNTA}}$ = –127.6 and $E_{\text{bind}}^{\text{ZnNTPA}}$ = –134.0 kcal mol^{-1}; hence, it consistently remains in favour of ZnNTPA, in this instance by –6.4 kcal mol^{-1}.

One can now reproduce the binding energy for each complex using a general purpose IQF expression shown in Eq. 12 where $\mathcal{G}$ and $\mathcal{H}$ stand for any two different molecular fragments,

$$E_{\text{bind}}^{\text{ML}} = \sum_{\mathcal{G}} E_{\text{def}}^{\mathcal{G}} + 0.5 \sum_{\mathcal{G}} \sum_{\mathcal{H} \neq \mathcal{G}} E_{\text{int}}^{\mathcal{G},\mathcal{H}} . \quad (12)$$

For convenience and clarity, first term in Eq. 12 can be expanded for our 4-fragment approach as

$$\sum_{\mathcal{G}} E_{\text{def}}^{\mathcal{G}} = (\Delta E_{\text{self}}^{\mathcal{L}} + \Delta E_{\text{int}}^{\mathcal{L}}) + (\Delta E_{\text{self}}^{\mathcal{M}} + \Delta E_{\text{int}}^{\mathcal{M}}) + (\Delta E_{\text{self}}^{(\mathcal{W}_1^{\text{o}})} + \Delta E_{\text{int}}^{(\mathcal{W}_1^{\text{o}})}) + (\Delta E_{\text{self}}^{(\mathcal{W}_2^{\text{o}})} + \Delta E_{\text{int}}^{(\mathcal{W}_2^{\text{o}})}) \quad (13)$$

where $\Delta E = E_{\text{c}} - E_{\text{p}}$ describes an energy contribution when a molecular fragment changed from pre-organized to in-complex state, and expressions in brackets (sum of self-fragment and intra-fragment interaction energies) are used for computing deformation energy of each fragment. The second term in Eq. 12 can be written as the sum of all unique inter-fragment interaction energies

$$0.5 \sum_{\mathcal{G}} \sum_{\mathcal{H} \neq \mathcal{G}} E_{\text{int}}^{\mathcal{G},\mathcal{H}} = E_{\text{int}}^{\mathcal{M}_{\text{c}},\mathcal{L}_{\text{c}}} + E_{\text{int}}^{\mathcal{M}_{\text{c}},(\mathcal{W}_1^{\text{o}})_{\text{c}}} + E_{\text{int}}^{\mathcal{M}_{\text{c}}(\mathcal{W}_2^{\text{o}})_{\text{c}}} + E_{\text{int}}^{\mathcal{L}_{\text{c}}(\mathcal{W}_1^{\text{o}})_{\text{c}}} + E_{\text{int}}^{\mathcal{L}_{\text{c}},(\mathcal{W}_2^{\text{o}})_{\text{c}}} + E_{\text{int}}^{(\mathcal{W}_1^{\text{o}})_{\text{c}},(\mathcal{W}_2^{\text{o}})_{\text{c}}} \quad (14)$$

Note that the energy terms, deformation, intra-fragment and self-fragment energies determined earlier for $\mathcal{L}_{\text{p}}$ (Table 8) are fully applicable in this instance. Furthermore, in case of a free metal ion, $E_{\text{def}}^{\mathcal{M}} = \Delta E_{\text{self}}^{\mathcal{M}}$ because the Zn^{2+} ion, as a separate molecular fragment, is not involved in intra-fragment interactions with itself, $\Delta E_{\text{int}}^{\text{Zn}} = 0$.

Table 9 shows that IQF-based analysis of 4-fragment partitioning scheme maintains the trend in the binding energy, –847.2 and –851.6 kcal mol^{-1} in ZnNTA and ZnNTPA, respectively. Even more importantly, $\Delta E_{\text{bind}}^{\text{ML}}$ = –4.4 kcal mol^{-1} in Table 9 recovers $\Delta E_{\text{bind}}^{\text{ML}}$ computed from electronic energies very well (Eq. 11). Except the bare metal ion that is stabilized, $E_{\text{def}}^{\mathcal{M}_{\text{f}}}$ = –203.5±2 kcal mol^{-1}, the deformation energy of each fragment is largely destabilizing. This can be explained by the changes in the electron populations. For $\mathcal{L}_{\text{p}}$, $(\mathcal{W}_1^{\text{o}})_{\text{p}}$ and $(\mathcal{W}_2^{\text{o}})_{\text{p}}$, there is an

outflow of electron density, $\Delta N < 0$, when they change to their in-complex state, $\mathcal{L}_c$, $(\mathcal{W}_1)_c$ and $(\mathcal{W}_2)_c$, as they donate density to the bare metal ion during complex formation. This resulted in the increase of these fragments self-energies and stabilizing in nature change in their intra-fragment interaction energy. In absolute term, the former is more significant than the latter,

Table 9. Energy components of E_{bind} (in kcal mol^{-1}), which were used in the interpretation of relative stability of ZnNTA and ZnNTPA complexes when 4-fragment partitioning scheme was used.

Energy term	ZnNTA	ZnNTPA	ΔE[a]
Fragments' deformation energy			
$E_{def}^{\mathcal{M}}$	–205.3	–201.6	3.7
$E_{def}^{\mathcal{L}}$	56.3	87.1	30.8
$E_{def}^{(\mathcal{W}_1)}$	39.0	42.7	3.7
$E_{def}^{(\mathcal{W}_2)}$	41.5	30.6	–10.9
Inter-fragment interaction energy			
$E_{int}^{\mathcal{M}_c,\mathcal{L}_c}$	–640.9	–675.9	–35.0
$E_{int}^{\mathcal{M}_c,(\mathcal{W}_1)_c}$	–49.6	–40.7	8.9
$E_{int}^{\mathcal{M}_c(\mathcal{W}_2)_c}$	–55.0	–38.6	16.4
$E_{int}^{\mathcal{L}_c(\mathcal{W}_1)_c}$	–16.2	–17.3	–1.1
$E_{int}^{\mathcal{L}_c,(\mathcal{W}_2)_c}$	–15.0	–35.7	–20.7
$E_{int}^{(\mathcal{W}_1)_c,(\mathcal{W}_2)_c}$	–2.0	–2.2	–0.2
E_{bind}	–847.2	–851.6	–4.4

[a] $\Delta E = E(\text{ZnNTPA}) - E(\text{ZnNTA})$

hence $E_{def}^{\mathcal{L}} > 0$. On the other hand, for both complexes $\mathcal{M}$ gained electron density, $\Delta N > 0$, donated by all the other fragments, resulting in a stabilized self-energy and hence highly stabilized deformation energy. Interestingly, the ligands consistently have attractive inter-fragment interaction energies with the water molecules and the inter-fragment interaction energy between water molecules in both complexes is also attractive. Similar to the Zn–O(w) coordination bonds' interaction energies, the inter-fragment $\mathcal{M}_c$•••$(\mathcal{W})_c$ interactions are more stabilizing in ZnNTA. This observation, in combination with deformation energies for water molecules (it amounts for about –18 kcal mol^{-1} in favour of ZnNTA) reaffirms our earlier conclusion drawn from electronic pre-organization and binding energies that water molecules play a decisive role in preferential complex formation between these two complexes.

3.2.6. Most Significant Contributions to Inter-fragment Interaction Energy

As shown in Table 9, the attractive interactions between the metal centre and the ligand make the most significant contribution to the binding energy in both complexes with $E_{\text{int}}^{\mathcal{M}_C,\mathcal{I}_C}$ being more significant for ZnNTPA by –35 kcal mol^{-1}. In search for the origin of this phenomenon, let us then focus on the most significant (de)stabilizing diatomic interactions involved. Individual interactions between Zn^{II} and all atoms in the ligand fragment in both complexes are shown in Table 10 (all other diatomic interactions which contribute to $E_{\text{int}}^{\mathcal{M}_C,\mathcal{I}_C}$ are shown in Tables S9-S15 in the SI). We note the following in both complexes:

(a) Interestingly and importantly, only the interactions of Zn with the N- and O-atoms (O(b) and O(nb)), are attractive.

(b) As expected, the coordination bonds show significant exchange-correlation contributions which amounts to about 20% of the interaction energy, $E_{\text{int}}^{\text{Zn,Y}}$, where Y = N, O(b). For the Zn•••O(nb) interactions, the XC-term is smaller than –1 kcal mol^{-1}.

(c) The Zn•••O(nb) stabilizing interactions play very important role as their energy contribution is about 55% of the $E_{\text{int}}^{\text{Zn,O(b)}}$ values.

(d) The coordination bonds of Zn to O(b)-atoms are more attractive in ZnNTPA, while all other interactions with negatively charged atoms, N- and O(nb)-atoms, are comparable in both complexes.

We have also analysed contributions made by α-, β- and γ-atoms to gain some insight on the significance of 5- and 6-membered rings in these complexes. Analysis of data in Table 10 leads to the following conclusions related to α-atoms:

- αC-atoms contribute in a destabilizing manner in both complexes and their contributions, $E_{\text{int}}^{\text{Zn,}\alpha\text{C}}$, are comparable.
- More significant total stabilizing contribution made by all α-atoms plus N-atoms in ZnNTPA, by about –20 kcal mol^{-1}, can be largely attributed to less repulsive interactions between αH-atoms and Zn^{II}, by about +3 kcal mol^{-1} per H-atom.

Considering β-atoms in ZnNTPA, the individual contributions made by C-atoms are negligible as they are orders of magnitude smaller when compared with αC and -γC-atoms. Furthermore, βH-atoms' contributions are comparable with αH-atoms in terms of their interactions with Zn^{II}. As a result, all β-atoms contributed just about +31 kcal mol^{-1}.

Table 10. IQA partitioning of two-bodied interaction energies (in kcal mol^{-1}) of all interactions between atoms of $\mathcal{L}$ and Zn^{II} in ZnNTPA and ZnNTA using the RXL3YP wavefunction on the MP2 structures.[a]

ZnNTPA					ZnNTA				
Atom Y	q^Y / e	$V_{cl}^{Zn,Y}$	$V_{XC}^{Zn,Y}$	$E_{int}^{Zn,Y}$	Atom Y	q^Y / e	$V_{cl}^{Zn,Y}$	$V_{XC}^{Zn,Y}$	$E_{int}^{Zn,Y}$
N4	–0.983	–221.1	–50.9	–272.0	N4	–1.020	–226.9	–46.3	–273.2
αC1	0.309	55.8	–0.9	54.9	αC1	0.304	57.2	–0.9	56.3
αH2	0.010	3.6	–0.2	3.4	αH2	0.030	6.0	–0.2	5.8
αH3	0.025	4.7	–0.1	4.6	αH3	0.045	7.8	–0.1	7.8
αC5	0.304	53.4	–0.7	52.8	αC5	0.288	54.7	–0.9	53.8
αH6	0.019	4.3	–0.1	4.2	αH6	0.035	6.6	–0.1	6.5
αH7	0.022	4.4	0.0	4.4	αH7	0.044	7.6	0.0	7.6
αC8	0.308	55.6	–1.0	54.6	αC8	0.300	56.2	–0.7	55.5
αH9	0.009	3.5	–0.2	3.3	αH9	0.033	6.3	–0.1	6.2
αH10	0.022	4.1	–0.3	3.8	αH10	0.045	7.7	0.0	7.7
***Sum*:**		***–31.7***	***–54.4***	***–86.0***	***Sum*:**		***–16.8***	***–49.3***	***–66.0***
βC11	0.014	2.1	–0.2	2.0					
βH12	0.024	4.0	0.0	4.0					
βH19	0.032	5.1	0.0	5.1					
βC13	0.017	2.5	–0.7	1.8					
βH14	0.021	4.4	0.0	4.4					
βH18	0.025	3.9	–0.4	3.6					
βC15	0.013	1.9	–0.5	1.4					
βH16	0.027	5.0	0.0	5.0					
βH17	0.025	4.1	–0.1	4.0					
***Sum*:**		***33.0***	***–1.9***	***31.3***					
γC20	1.579	245.0	–0.8	244.2	γC11	1.590	249.0	–0.8	248.2
O21(nb)	–1.244	–140.1	–0.6	–140.7	O12(nb)	–1.239	–139.1	–0.5	–139.5
O22(b)	–1.223	–258.6	–52.5	–311.1	O13(b)	–1.212	–251.5	–48.8	–300.2
γC23	1.577	236.7	–0.7	236.1	γC14	1.593	249.7	–0.9	248.8
O24(nb)	–1.243	–135.8	–0.5	–136.3	O16(nb)	–1.241	–139.3	–0.5	–139.8
O25(b)	–1.229	–256.6	–50.2	–306.8	O15(b)	–1.216	–252.2	–48.6	–300.8
γC26	1.567	240.1	–0.7	239.4	γC17	1.596	251.6	–0.9	250.7
O27(nb)	–1.241	–137.6	–0.5	–138.1	O18(nb)	–1.240	–139.9	–0.5	–140.3
O28(b)	–1.229	–257.0	–50.9	–307.9	O19(b)	–1.220	–253.6	–48.3	–301.9
$\sum E_{int}^{Zn,\gamma(C)}$		*721.8*	*–2.2*	*719.7*	$\sum E_{int}^{Zn,\gamma(C)}$		*750.3*	*–2.6*	*747.7*
$\sum E_{int}^{Zn,O(nb)}$		*–413.5*	*–1.6*	*–415.1*	$\sum E_{int}^{Zn,O(nb)}$		*–418.3*	*–1.5*	*–419.6*
$\sum E_{int}^{Zn,O(b)}$		*–772.2*	*–153.6*	*–925.8*	$\sum E_{int}^{Zn,O(b)}$		*–757.3*	*–145.7*	*–902.9*
***Sum*:**		***–463.9***	***–157.4***	***–621.2***	***Sum*:**		***–425.3***	***–149.8***	***–574.8***
Total:		**–462.1**	**–213.8**	**–675.9**	**Total:**		**–441.9**	**–199.0**	**–640.9**

[a] q^{Zn} in NTPA is +1.362e and in NTA is +1.355e.

Focusing on -γ-atoms, we found:

- The repulsive interactions of Zn^{II} with the γC-atoms of the carboxylate groups are (i) about 5-times more destabilizing than those with the αC atoms in both complexes and importantly (i)

more severe in ZnNTA, in total by about +28 kcal mol^{-1}; note that this is comparable with the total β-atoms' contributions in ZnNTPA.

- The sum of $E_{\text{int}}^{\text{Zn,O(b)}}$ terms is more significant in ZnNTPA, by about –24 kcal mol^{-1}, whereas sum of $E_{\text{int}}^{\text{Zn,O(nb)}}$ terms is comparable in both complexes.

Importantly, we also see the manifestation of the inductive effect in the binding step and how it influences the relative values of the binding energy; in general, the trend is identical to that found for the Be$^{\text{II}}$ complexes.[14] The presence of the additional fragment –CH_2– in NTPA results in increased density of atoms in the neighbouring region, αH- and γC-atoms. These atoms have less positive charges than the analogous atoms in NTA, and O(b)-atoms have more negative charges in NTPA. This results in the electrostatic terms being less repulsive with the backbone of the NTPA ligand and having far more attractive coordination bonds. Thus, the inter-fragment interaction energy, and by extension the binding, is overly more attractive for NTPA.

It is seen in Table 10 that the second largest relative stabilizing contribution to $\Delta E_{\text{bind}}^{\text{ML}}$ came from interactions between a ligand $\mathcal{L}_{\text{c}}$ and an axial water molecule, $(\mathcal{W}_2^a)_{\text{c}}$. It was then of interest to learn about the origin of $E_{\text{int}}^{\mathcal{L}_{\text{c}},(\mathcal{W}_2^a)_{\text{c}}}$(ZnNTPA) $-E_{\text{int}}^{\mathcal{L}_{\text{c}},(\mathcal{W}_2^a)_{\text{c}}}$(ZnNTA) = –20.7 kcal mol^{-1}. To achieve that, we summed the most significant stabilizing and destabilizing interactions, between atoms of $(\mathcal{W}_2^a)_{\text{c}}$ and atoms of $\mathcal{L}_{\text{c}}$ (Table S9 in the SI), such that their overall contribution approximated –20.7 kcal mol^{-1}. This allowed us to eliminate all interactions of no significance and we were left with α- and γ-atoms in in both ligands. Next, we grouped interactions between atoms of axial water molecule $(\mathcal{W}_2^a)_{\text{c}}$ with specific atoms of the ligand and results obtained are shown in Table 11. It reveals several consistent and informative trends in both complexes:

a) Interactions with N-atom as well as αC-atoms of $\mathcal{L}_{\text{c}}$ are almost identical; hence, main (de)stabilizing contributions came from interactions with atoms of carboxylate group.

b) $\left|E_{\text{int}}^{\text{H(w),O(b)}}\right| > \left|E_{\text{int}}^{\text{O(w),}\gamma\text{C}}\right| >> \left|E_{\text{int}}^{\text{H(w),O(nb)}}\right|$ for most stabilizing contributions.

c) $E_{\text{int}}^{\text{H(w),}\gamma\text{C}} > E_{\text{int}}^{\text{O(w),O(b)}} >> E_{\text{int}}^{\text{O(w),O(nb)}}$ for most destabilizing contributions.

The combined contribution made by most significant interaction energies gave –21.2 kcal mol^{-1} in favour of ZnNTPA. This compares with $\Delta E_{\text{int}}^{\mathcal{L}_{\text{c}},(\mathcal{W}_2^a)_{\text{c}}}$ of –20.7 kcal mol^{-1} (see Table 9) very well and validates approach taking here. It allowed us to pin-point at interactions between H-atoms of axial water molecule and O(b) atoms of NTPA as mainly responsible for more favourable interaction between $(\mathcal{W}_2^a)_{\text{c}}$ and NTPA relative to NTA. All the above provides an

invaluable and descriptive picture of the nature and significance of interactions discussed here, which also agrees with common sense. Note that interactions with N- and α-atoms are several times weaker when compared with γ-atoms and this is because the axial water molecule is much closer to atoms of carboxylate functional group.

Table 11. Analysis of interaction energies between atoms X of axial water $(\mathcal{W}_2^e)_c$ and atoms Y of $\mathcal{L}_c$ in both complexes. All values in kcal mol^{-1}.

ZnNTA			ZnNTPA			$\Delta E_{int}^{X,Y}$ [a]
Atom X	**Atom Y**	$E_{int}^{X,Y}$	**Atom X**	**Atom Y**	$E_{int}^{X,Y}$	
H23/H24	N4	–91.2	H32/H33	N4	–88.8	2.4
O22		91.7	O31		87.4	4.3
	Total:	**0.5**		**Total:**	**–1.4**	**–1.9**
H23/H24	αC1/5/8	75.3	H32/H33	αC1/5/8	75.9	0.6
O22		–75.3	O31		–74.3	1.0
	Total:	**0.0**		**Total**	**1.6**	**1.6**
H23/H24	γC11/14/17	432.7	H32/H33	γC20/23/26	469.7	37.0
O22		–426.4	O31		–449.5	–23.1
	Total:	**6.3**		**Total:**	**20.2**	**13.9**
H23/H24	O13/15/19(b)	–429.8	H32/H33	O22/25/28(b)	–484.4	–54.6
O22		416.3	O31		443.7	27.4
	Total:	**–13.5**		**Total:**	**–40.7**	**–27.2**
H23/H24	O12/16/18(nb)	–276.3	H32/H33	O21/24/27(nb)	–306.9	–30.6
O22		268.0	O31		291.0	23.0
	Total:	**–8.3**		**Total:**	**–15.9**	**–7.6**
					Total:	***–21.2***

[a] $\Delta E_{int}^{X,Y} = E_{int}^{X,Y}(\text{NTPA}) - E_{int}^{X,Y}(\text{NTA})$.

4. Conclusions

The understanding of the relative stability of molecular systems is at the core of all chemistry. In coordination chemistry, trends observed in so-called Linear Free Energy Relationships were used as a predictive tool in relative stability of metal complexes. The main drawback of this classical approach is the fact that no insight on the fundamental origin can be obtained.

As also found in our previous studies on BeII complexes,[14] the analysis of individual properties yielded interesting results and provided fascinating insight into properties of these metal complexes, but it (i) still failed to explain the preferential formation of ZnNTA, (ii) generated many, but mainly, contradictory trends and (iii) interaction energies attributed to the coordination bonds uncovered that average size Zn^{II} ion also shows higher affinity to NTPA

even though a reverse trend in complex stability applies. This stipulates, contrary to common notion, that strength of coordination bonds to NTA and NTPA ($\mathcal{L}$) is not necessarily related to the size of a metal ion or geometry of coordination rings.

We found that Zn^{II} interacts stronger with water molecules in ZnNTA and only summing up all interaction energies $E_{\text{int}}^{\text{Zn,X}}$, (X = N- and O-donor atoms) produced relative difference in favour of ZnNTA, by about –12 kcal mol^{-1}, in accord with the experimental trend.

We have also investigated repulsion between free pairs of electrons in the coordination sphere as it is commonly used in predicting relative stability of metal complexes. We found that interaction energies just between donor atoms amount to +2019 kcal mol^{-1} in ZnNTA which is over 24 kcal mol^{-1} larger when compared with ZnNTPA. From this perspective, NTA appears to be more strained which is in direct conflict with classical interpretation. More importantly, these repulsive contributions override the energy generated by attractive coordination bonds by over +300 kcal mol^{-1} in both complexes. Furthermore, IQA-based extensive analysis of the CH--HC contacts in coordination sphere of $\mathcal{L}$ revealed that, contrary to previous reports[1,5] they are not strained and, in general, their energetic contribution is of no importance at all.

It became clear that some other and of stabilizing nature contributions are not accounted for, otherwise these complexes would not form. Hence, we decided to apply 2- and 4-fragment partitioning schemes and make use of IQF concepts as implemented in the π-FARMS methodology.[14]

Using computed electronic pre-organisation energies of water-containing fragment, $\mathcal{M}_{\text{w}}$ = $[Zn(H_2O)_2]^{2+}$, and ligand as the second fragment, $\mathcal{L}$, we found:

a) $E_{\text{p-org}}^{\text{NTPA}} > E_{\text{p-org}}^{\text{NTA}}$ with pre-organization energy (strain) of NTPA being larger by about 11.5 kcal mol^{-1} in accord with general knowledge; the same trend was also found for the Ni^{II} [11] and Be^{II} complexes.[14]

b) $E_{\text{p-org}}^{\mathcal{M}_{\text{w}}}(\text{NTPA}) > E_{\text{p-org}}^{\mathcal{M}_{\text{w}}}(\text{NTA})$ showing that the $(\mathcal{M}_{\text{w}})_{\text{p}}$ fragment binding to NTPA acquired greater strain by about 6.1 kcal mol^{-1} which is in general agreement with ETS-NOCV studies.[13]

c) Affinity of Zn^{II} to NTPA, as measured by the binding energy $E_{\text{bind}}^{\text{ZnNTPA}}$, is more favourable by –12.4 kcal mol^{-1}, which is consistent with the computed strengths of coordination bonds with $\mathcal{L}$.

d) Accounting just for strain in $\mathcal{L}$ and binding between Zn^{II} and $\mathcal{L}$ is not sufficient to recover relative stability of complexes as $E_{\text{bind}}^{\text{ZnNTPA}} + E_{\text{p-org}}^{\text{NTPA}} \approx E_{\text{bind}}^{\text{ZnNTA}} + E_{\text{p-org}}^{\text{NTA}}$.

e) $(E_{\text{p-org}}^{\mathcal{M}_w}(\text{NTPA}) + E_{\text{p-org}}^{\text{NTPA}} + E_{\text{bind}}^{\text{ZnNTPA}})$ < $(E_{\text{p-org}}^{\mathcal{M}_w}(\text{NTA}) + E_{\text{p-org}}^{\text{NTA}} + E_{\text{bind}}^{\text{ZnNTA}})$ by 5.2 kcal mol^{-1}; this is in excellent agreement with the energy differences computed from the $\log K_1$ values and fully supports our notion that coordinated water molecules play an important, if not decisive role in controlling relative complex stability.

Where applicable, exactly the same trends were obtained from the 4-fragment partitioning scheme. Moreover, we conducted dedicated IQA/IQF-based studies from which we established that the origin of:

a) Pre-organization (strain) energy of ligands $\mathcal{L}$ cannot be linked with α-atoms in both $\mathcal{L}$ or β-atoms of NTPA; their additive atomic and interaction energy with remaining atoms of the ligands changed marginally and this contradicts a common view that the intramolecular CH--HC contacts are destabilizing in NTPA.

b) The main source of intra-ligand strain is mainly caused by O-atoms of the carboxylate groups in both ligands. Their additive atomic energies contributed +28.7 and +57.6 kcal mol^{-1} per a single coordinating arm in NTA and NTPA, respectively which correlates with the trend in pre-organization energy. Furthermore, larger strain in NTPA has been confirmed by the larger deformation energy term, $E_{\text{def}}^{\text{NTPA}}$, by about +31 kcal mol^{-1}. Interestingly, C-atoms of carboxylate group add to stability of both ligands but their contribution has not changed the computed trend, $E_{\text{p-org}}^{\text{NTPA}} > E_{\text{p-org}}^{\text{NTA}}$.

c) Strain energy of metal-containing fragments, $\mathcal{M}_w$, can be attributed to metal centre itself. Both energy terms, self-atomic and interaction energy between Zn^{II} and remaining atoms of $\mathcal{M}_w$, increased and more, by about 20 kcal mol^{-1}, for $(\mathcal{M}_w)_{\text{ZnNTPA}}$. We also discovered that in both $\mathcal{M}_w$ fragments H-atoms of equatorial water molecule became stabilized whereas all atoms of axial water molecules became destabilized in both $\mathcal{M}_w$ fragments. Importantly these (de)stabilizing contributions virtually cancelled out and our analysis fully confirmed the $E_{\text{p-org}}^{\mathcal{M}_w}(\text{NTPA}) > E_{\text{p-org}}^{\mathcal{M}_w}(\text{NTA})$ trend with pin-pointing at Zn^{II} as a main contributor.

d) Preferential binding energy (from 2-fragment partitioning scheme) can be entirely attributed to the inter-fragment interaction energy term, $E_{\text{int}}^{(\mathcal{M}_w)_c, \mathcal{L}_c}$, which was found to be more favourable in ZnNTPA, by –56.7 kcal mol^{-1}. The origin of more favourable (more negative)

$E_{\text{int}}^{(\mathcal{M}_{\text{w}})_{\text{c}},\mathcal{I}_{\text{c}}}$ in case of ZnNTPA is the result of more stabilizing contribution of interaction energy between Zn^{II} and O(b) (by about –17 kcal mol^{-1}) and more repulsive interactions in ZnNTA between Zn^{II} and C-atoms of carboxylate groups, by about +28 kcal mol^{-1}.

This second successful application of the π-FARMS methodology gives us confidence that it is of general nature; hence, it should be possible to investigate any metal-containing compounds (organometallics) or metal-free compounds either in their equilibrium or transitional state which opens up a new avenue of applications, among others in understanding reaction mechanisms.

ASSOCIATED CONTENT

Supporting Information.

Protocol for determining the equilibrium constants for competition reactions, QTAIM and NCI explanations of the preorganization of ligand fragments, derivation of the IQF-rooted π-FARMS methodology as applied to complexes discussed in this work. In additional Molecular graphs, topological properties and Interacting Quantum Atoms interaction energies are presented.

AUTHOR INFORMATION

Corresponding Author: *E-mail: ignacy.cukrowski@up.ac.za

Notes

The authors declare no competing financial interest.

ACKNOWLEDGMENT

This work is based on the research supported in part by the National Research Foundation of South Africa (Grant Numbers 87777) and the University of Pretoria.

ABBREVIATIONS

QTAIM, Quantum Theory of Atoms in Molecules; NCI, Non-Covalent Interactions; IQA, Interacting Quantum Atoms; IQF, Interacting Quantum Fragments; π-FARMS, Preorganized-interacting Fragment Attributed Relative Molecular Stability; AIL, Atomic Interaction Line; BP, Bond Path; NTA, Nitrilotriacetic acid; NTPA, Nitrilotri-3-propionic acid; ZnNTA, $[Zn^{II}NTA(H_2O)_2]^-$; ZnNTPA, $[Zn^{II}NTPA(H_2O)_2]^-$; CRn, Competition Reaction; LEC, Lowest Energy Conformer;

References

[1] Martell, A. E.; Hancock, R. D. *Metal Complexes in Aqueous Solutions*, Plenum Press: New York, 1996.

[2] Hancock, R. D. *Acc. Chem. Res.***1990**, *23*, 253–257

[3] Thom, V. J., Fox, C. C., Boeyens, J. C. A., Hancock, R. D. *J. Am. Chem. Soc.***1984**, *106*, 5947–5955.

[4] Hambley, T. W. *J. Chem. Soc., Dalton Trans.* **1986**, 565–569.

[5] Hancock, R.D., Nikolayenko, I.V. *J. Phys. Chem. A.* **2012**, *116*, 8572−8583

[6] Hancock, R.D. *Chem. Soc. Rev.* **2013**, *42*, 1500–1524.

[7] Mitoraj, M. P., Michalak, A., Ziegler, T. *J. Chem. Theory Comput.* **2009**, *5*, 962–975.

[8] Mitoraj, M. P., Michalak, A., Ziegler, T. *Organometallics* **2009**, *28*, 3727–3733.

[9] Mitoraj, M. P. *J. Phys. Chem. A* **2011**, *115*, 14708-14716.

[10] Varadwaj, P. R., Varadwaj, A., Peslherbe, G. H., Marques, H. M. *J. Phys. Chem. A.* **2011**, *115*, 13180–13190.

[11] Govender, K.K., Cukrowski, I. *Inorg. Chem.* **2010**, *49*, 6931–6941.

[12] Cukrowski, I., Matta, C. *Chemical Physics Letters* **2010**, *499*, 66–69.

[13] Cukrowski, I., Govender, K.K., Mitoraj, M., Srebro, M. *J. Phys. Chem. A.* **2011**, *115*, 12746–12757.

[14] I. Cukrowski, I., Mangondo, P. *J. Comp. Chem*, 2016, *37*, 1373–1387.

[15] Pendás, A. M., Blanco, M. A., Francisco, E. *J. Chem. Phys.* **2006**, *125*, 184112– 184119.

[16] NIST Standard Reference Database 46. NIST Critically Selected Stability Constants of Metal Complexes Database, version 8.0; Database collected and selected by R. M.Smith, US Department of Commerce, National Institute of Standards and Technology: Gaithersburg, MD, 2004.

[17] Blanco, M. A., Pendás, A. M., Francisco, E. *J. Chem. Theory Comput.* **2005**, *1*, 1096−1109.

[18] Francisco, E., Pendás, A. M., Blanco, M. A. A. *J. Chem. Theory Comput.* **2006**, *2*, 90−102.

[19] Pendás, A. M., Blanco, M. A., Francisco, E. *J. Comput. Chem.* **2006**, *28*, 161−184.

[20] Pendás, A. M., Blanco, M. A., Francisco, E. *J. Comp. Chem.* **2009**, *30*, 98–109.

[21] M. J. Frisch, G. W. Trucks, H. B. Schlegel, G. E. Scuseria, M. A. Robb, J. R. Cheeseman, G. Scalmani, V. Barone, B. Mennucci, G. A. Petersson, H. Nakatsuji, M. Caricato, X. Li, H. P. Hratchian, A. F. Izmaylov, J. Bloino, G. Zheng, J. L. Sonnenberg, M. Hada, M. Ehara, K. Toyota, R. Fukuda, J. Hasegawa, M. Ishida, T. Nakajima, Y. Honda, O. Kitao, H. Nakai, T. Vreven, J. A. Montgomery, Jr., J. E. Peralta, F. Ogliaro, M. Bearpark, J. J. Heyd, E. Brothers, K. N. Kudin, V. N. Staroverov, R. Kobayashi, J. Normand, K. Raghavachari, A. Rendell, J. C. Burant, S. S. Iyengar, J. Tomasi, M. Cossi, N. Rega, J. M. Millam, M. Klene, J. E. Knox, J. B. Cross, V. Bakken, C. Adamo, J. Jaramillo, R. Gomperts, R. E. Stratmann, O. Yazyev, A. J. Austin, R. Cammi, C. Pomelli, J. W. Ochterski, R. L. Martin, K. Morokuma, V. G. Zakrzewski,

G. A. Voth, P. Salvador, J. J. Dannenberg, S. Dapprich, A. D. Daniels, Ö. Farkas, J. B. Foresman, J. V. Ortiz, J. Cioslowski, and D. J. Fox, Gaussian 09, Revision D.1, Gaussian, Inc., Wallingford CT, 2013.

[22] Bader, R. W. F. Atoms in Molecules: A Quantum Theory, Oxford University Press: Oxford, U.K., 1990.

[23] Keith, A. AIMAll (Version 13.11.04), TK Gristmill Software, Overland Parks KS, USA, 2013 (aim.tkgristmill.com).

[24] Maxwell, P., Pendás, A. M., Popelier, P. L. A. *PCCP*, **2016**, DOI: 10.1039/c5cp07021j.

[25] Tognetti, V., Joubert, L. *J. Chem. Phys.* **2013**, *138*, 024102–024108.

[26] Johnson, E. R., Keinan, S., Mori-Sánchez, P., Contreras-García, J., Cohen, A. J., Yang, W. *J. Am. Chem. Soc.* **2010**, *132*, 6498−6506.

[27] Contreras-García, J., Johnson, E. R., Keinan, S., Chaudret, R., Piquemal, J. P., Beratan, D., Yang, W. *J. Chem. Theory Comput.* **2011**, *7*, 625−632.

[28] N. Gillet, R. Chaudret, J. Contreras-García, W. Yang, B. Silvi, J. P. Piquemal, *J. Chem. Theory Comput.* **2012**, *8*, 3993−3997.

[29] Contreras-García, J., Yang, W., Johnson, E. R. *J. Phys. Chem. A* **2011**, *115*, 12983−12990.

[30] Xu, X., Goddard, W. A. *Proc. Natl. Acad. Sci.* USA, **2004**, *101*, 2673–2677.

[31] Perdew, J. P., Burke, K., Ernzerhof, M. *Phys. Rev. Lett.* **1996**, *77*, 3865–3868.

[32] Hyla-Kryspin, I., Haufe, G., Grimme, S. *Chem. Eur. J.* **2004**, *10*, 3411–3422.

[33] Hammer, B., Hansen, L. B., Nørskov, J. K. *Phys. Rev. B* **1999**, *59*, 7413–7421.

[34] Bader, R. F. W. *J. Phys. Chem. A* **2009**, *113*, 10391–10396.

[35] Foroutan-Nejad, C., Shahbazian, S., Marek, R. *Chem. Eur. J.* **2014**, *20*, 10140 – 10152.

[36] Cukrowski, I., de Lange, J. H., Adeyinka, A. S., Mangondo, P. *Comput. Theoret. Chem.* **2015**, *1053*, 60–76.

[37] Rafat, M., Popelier, P. L. A. Chapter 5 in The Quantum Theory of Atoms in Molecules, eds. Matta, C. F. and Russell J. Boyd, R. J., WILEY-VCH Verlag GmbH & Co. KGaA, Weinheim, **2007**, pp. 121–140.

[38] Badri, Z., Cina Foroutan-Nejad, C., Kozelka., J., Marek, M. *Phys. Chem. Chem. Phys.*, **2015**, *17*, 26183–26190.

[39] Foroutan-Nejad, C., Badri, Z., Marek,R. *Phys. Chem. Chem. Phys.*, **2015**, *17*, 30670–30679.

[40] Badri, Z., Foroutan-Nejad, C. *Phys. Chem. Chem. Phys.*, **2016**, *18*, 11693–11699.